AD-A078 517 ANALYTIC SCIENCES CORP READING MA F/G 17/7
DIFFERENTIAL OMEGA IN THE ALASKA/YUKON REGION: AN ANALYTIC ASSE--ETC(U)
AUG 79 J M FOLTZ , B E GRIFFITHS , R D HEALY DOT-FA78WA-4236
UNCLASSIFIED TASC-TR-1579-1 FAA-RD-79-77 NL

| OF |
AD-
A078517

END
DATE FILMED
1-80
DDC

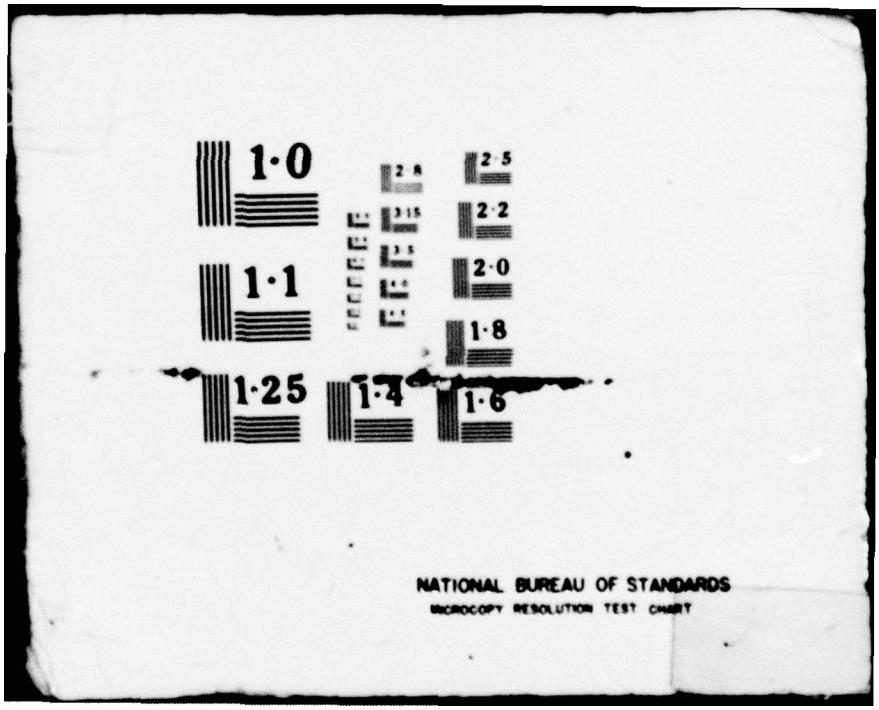
1·0
1·1
1·25
1·4
1·6
1·8
2·0
2·2
2·5
NATIONAL BUREAU OF STANDARDS
MICROCOPY RESOLUTION TEST CHART

REPORT NO. FAA-RD-79-77

12 LEVEL II

DIFFERENTIAL OMEGA IN THE ALASKA/YUKON REGION: AN ANALYTIC ASSESSMENT

JAMES M. FOLTZ
BARRY E. GRIFFITHS
RICHARD D. HEALY
RADHA R. GUPTA

THE ANALYTIC SCIENCES CORPORATION
Six Jacob Way
Reading, Massachusetts 01867

August 1979

FINAL REPORT

Prepared for

U.S. DEPARTMENT OF TRANSPORTATION
FEDERAL AVIATION ADMINISTRATION
Systems Research & Development Service
Washington, D.C. 20590

NOTICE

This document is disseminated under the sponsorship of the Department of Transportation in the interest of information exchange. The United States Government assumes no liability for its contents or use thereof.

Technical Report Documentation Page

1. Report No.	2. Government Accession No.	3. Recipient's Catalog No.
FAA-RD-79-77		

4. Title and Subtitle
Differential Omega in the Alaska/Yukon Region: An Analytic Assessment.

5. Report Date
Aug [redacted] 79

6. Performing Organization Code

7. Author(s)
J.M. Foltz, E. Griffiths, D. Healy, R. Gupta

8. Performing Organization Report No.
TR-1579-1

9. Performing Organization Name and Address
The Analytic Sciences Corporation
Six Jacob Way
Reading, Massachusetts 01867

10. Work Unit No. (TRAIS)

11. Contract or Grant No.
DOT-FA78WA-4236

12. Sponsoring Agency Name and Address
Systems Research and Development Service
Federal Aviation Administration
Washington, D.C. 20591

13. Type of Report and Period Covered
Final Report
Oct [redacted] 78 — Jul[redacted] 79

14. Sponsoring Agency Code
FAA/ARD-732

15. Supplementary Notes
TASC-TR-1579-1

16. Abstract

This report presents an analytic evaluation of the differential Omega experiment being conducted by the Federal Aviation Administration in the Alaska/Yukon region. An error model for Omega propagation prediction residuals is used to predict performance achievable with an equipment suite consisting of a TRACOR 599R Omega monitor receiver and associated ground station equipment built by Transport Canada, and an airborne suite which includes a modified TRACOR 7620 Omega navigation set and special-purpose differential Omega equipment built by Systems Control, Inc. (Vt.). Predictions are made for use of the equipment as a non-precision approach aid within the differential Omega coverage area and for use as an enroute navigation aid between areas serviced by a differential Omega ground station.

17. Key Words	18. Distribution Statement
differential Omega VLF navigation area navigation non-precision approach	This document is available to the U.S. public through the National Technical Information Service, Springfield, Virginia 22161.

19. Security Classif. (of this report)	20. Security Classif. (of this page)	21. No. of Pages	22. Price
Unclassified	Unclassified	94	

Form DOT F 1700.7 (8-72) Reproduction of completed page authorized

AD A104 565

METRIC CONVERSION FACTORS

Approximate Conversions to Metric Measures

Symbol	When You Know	Multiply by	To Find	Symbol
	LENGTH			
in	inches	*2.5	centimeters	cm
ft	feet	30	centimeters	cm
yd	yards	0.9	meters	m
mi	miles	1.6	kilometers	km
	AREA			
in^2	square inches	6.5	square centimeters	cm^2
ft^2	square feet	0.09	square meters	m^2
yd^2	square yards	0.8	square meters	m^2
mi^2	square miles	2.6	square kilometers	km^2
	acres	0.4	hectares	ha
	MASS (weight)			
oz	ounces	28	grams	g
lb	pounds	0.45	kilograms	kg
	short tons (2000 lb)	0.9	tonnes	t
	VOLUME			
tsp	teaspoons	5	milliliters	ml
Tbsp	tablespoons	15	milliliters	ml
fl oz	fluid ounces	30	milliliters	ml
c	cups	0.24	liters	l
pt	pints	0.47	liters	l
qt	quarts	0.95	liters	l
gal	gallons	3.8	liters	l
ft^3	cubic feet	0.03	cubic meters	m^3
yd^3	cubic yards	0.76	cubic meters	m^3
	TEMPERATURE (exact)			
°F	Fahrenheit temperature	5/9 (after subtracting 32)	Celsius temperature	°C

*1 in = 2.54 (exactly). For other exact conversions and more detailed tables, see NBS Misc. Publ. 286, Units of Weights and Measures, Price $2.25, SD Catalog No. C13.10:286.

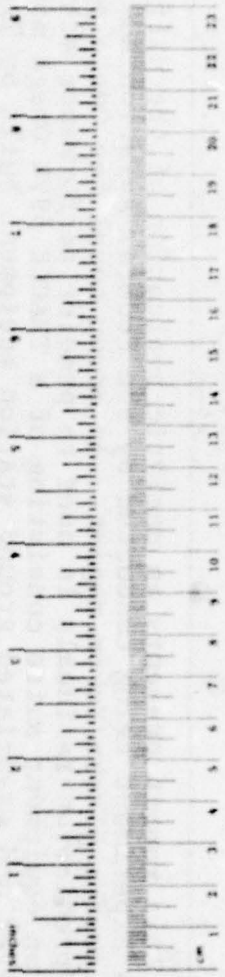

Approximate Conversions from Metric Measures

Symbol	When You Know	Multiply by	To Find	Symbol
	LENGTH			
mm	millimeters	0.04	inches	in
cm	centimeters	0.4	inches	in
m	meters	3.3	feet	ft
m	meters	1.1	yards	yd
km	kilometers	0.6	miles	mi
	AREA			
cm^2	square centimeters	0.16	square inches	in^2
m^2	square meters	1.2	square yards	yd^2
km^2	square kilometers	0.4	square miles	mi^2
ha	hectares (10,000 m^2)	2.5	acres	
	MASS (weight)			
g	grams	0.035	ounces	oz
kg	kilograms	2.2	pounds	lb
t	tonnes (1000 kg)	1.1	short tons	
	VOLUME			
ml	milliliters	0.03	fluid ounces	fl oz
l	liters	2.1	pints	pt
l	liters	1.06	quarts	qt
l	liters	0.26	gallons	gal
m^3	cubic meters	35	cubic feet	ft^3
m^3	cubic meters	1.3	cubic yards	yd^3
	TEMPERATURE (exact)			
°C	Celsius temperature	9/5 (then add 32)	Fahrenheit temperature	°F

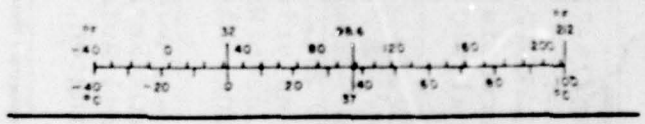

TABLE OF CONTENTS

TABLE OF CONTENTS (Continued)

LIST OF FIGURES

LIST OF FIGURES (Continued)

LIST OF TABLES

LIST OF TABLES (Continued)

1. INTRODUCTION

1.1 OVERVIEW

The Federal Aviation Administration (FAA) is investigating the feasibility of using differential Omega as a solution to general aviation user requirements in the Alaska region. At present, a feasibility demonstration experiment is being conducted in the Alaska/Yukon region. The experiment is a joint venture between the U.S. Department of Transportation and the Canadian Ministry of Transport.

Differential Omega is a concept for improving the navigation performance of airborne equipment in the vicinity of a fixed-site ground station. The Omega Navigation System is a worldwide Very-Low-Frequency (VLF) radio navigation aid (Ref. 1). Because the errors associated with Omega are highly correlated in space (Ref. 2), a single monitor station can service a relatively large area (ranges well in excess of 100 nm from the monitor). Basic Omega coverage in Alaska is good: signals from at least four Omega transmitting stations are normally available (Ref. 3). Therefore, differential Omega offers a potential cost-effective alternative to establishing a network of VOR/DME* stations in Alaska (Refs. 3 and 4).

The current differential Omega experiment involves several participants. The experiment coordinator is the Systems Research and Development Service, FAA. Ground station equipment

---

*Very-High-Frequency Omnidirectional Range (VOR) and Distance-Measuring Equipment (DME) are the primary aids for enroute navigation in the continental U.S.

was built by Transport Canada. Airborne equipment is installed in FAA aircraft. Airborne data equipment was built by Systems Control, Inc. (Vt.) (SCI), and data are being collected by SCI. The airborne navigation receiver equipment was manufactured by TRACOR, Inc.

The Analytic Sciences Corporation (TASC) was tasked by the FAA to perform an analytic evaluation of the experiment in order to:

- Determine whether the experimental differential Omega system can meet certification requirements as a non-precision approach aid
- Determine the suitability of the Omega receiver as an enroute navigation aid
- Define primary requirements for equipment suitable for certification as a non-precision approach aid and for enroute navigation.

This report presents the results of these analyses.

1.2 DESCRIPTION OF THE EXPERIMENT

The differential Omega concept is illustrated in Fig. 1. Omega navigation signals are received simultaneously by an airborne receiver and a ground station monitor. At the ground station, the received signal is compared with a nominal value and a correction is computed. The correction is uplinked to the aircraft using an audio signal superimposed on a Non-Directional Beacon (NDB). Airborne equipment decodes the telemetry message and applies the correction to improve navigation accuracy.

For the Alaska/Yukon experiment, three NDBs have been selected for instrumentation as ground stations: CHENA at

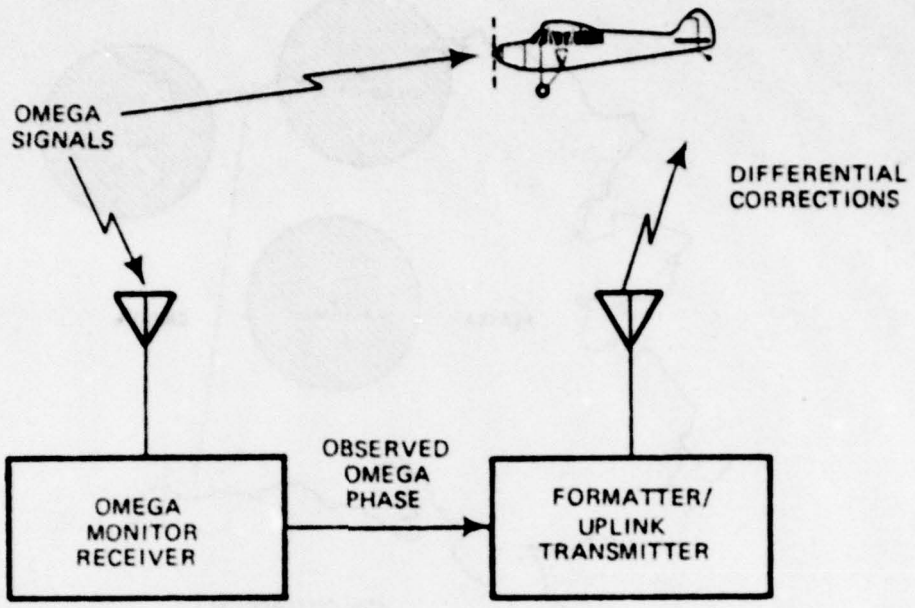

Figure 1 The Differential Omega Concept

Fairbanks, Alaska; *INUVIK at Inuvik*, Northwest Territories; and PUT RIVER at Deadhorse, Alaska. The NDB signal has a usable range of about 125 nm and the relative geometry is depicted in Fig. 2.

Ground station equipment consists of TRACOR 599R Omega monitor receivers, a specially designed signal processor, and recording equipment. The receivers have been modified to provide digital output of phase and signal amplitude, and atomic frequency standards are used as reference oscillators. The differential correction message format is summarized in Table 1.

Airborne equipment consists of an interface adapter/message decoder for receiving the correction message, a TRACOR 7620 Omega navigation set, recording equipment, and true airspeed and stabilized heading inputs to the navigation set. The

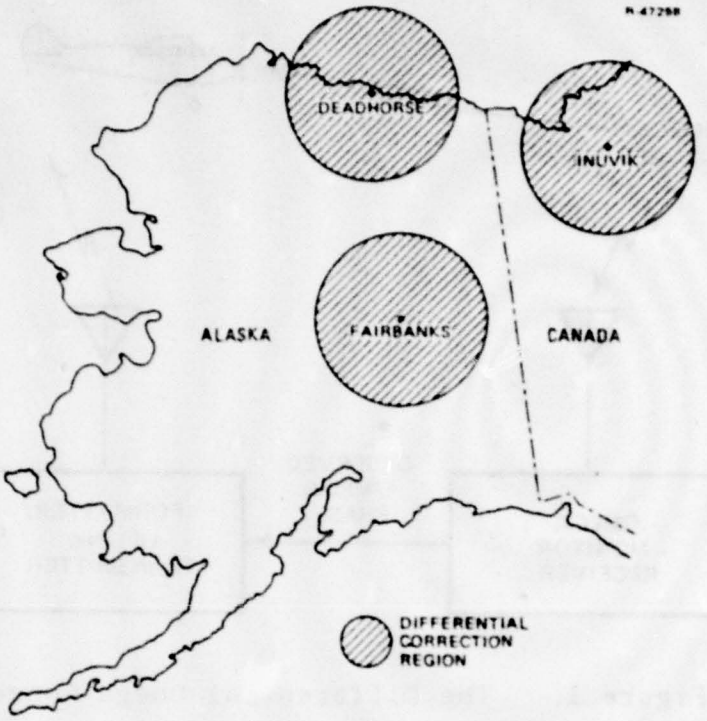

Figure 2 Geographical Relationship of the Ground Stations

TABLE 1

DIFFERENTIAL CORRECTION MESSAGE FORMAT

Header
Byte Count
Station Identification
Four channels of 10.2 kHz data
Four channels of 13.6 kHz data
Four channels of 11.33 kHz data
Signal Quality at 10.2 kHz
Signal Quality at 13.6 kHz
Signal Quality at 11.33 kHz
Checksum

airborne receiver has been modified to accept the differential corrections instead of computing Omega propagation corrections*.

1.3 REPORT ORGANIZATION

This report is organized into five chapters and three appendices. Chapter 1 is an introduction to the report and provides an overview of the experiment. Chapter 2 presents the essential features of the models used to evaluate the per- of the TRACOR 7620 navigation set and the differential Omega concept. Details of the Omega models are described in Appendices A and B.

Analytical predictions for the differential Omega system are presented in Chapter 3. Section 3.2 describes application as a non-precision approach aid, and Section 3.3 describes application as an enroute aid. Section 3.2 contains analyses which evaluate the sensitivity of the performance predictions to uncertainties in model parameters and modeling assumptions. Additional details of the TRACOR 7620 mechanization are contained in Appendix C.

Chapter 4 contains an analysis of the performance predictions in terms of their implications for certification of the differential Omega equipment. The results are presented with reference to three separate criteria: certification requirements, user requirements, and procedural requirements. The criteria are defined in Section 4.1.

Chapter 5 summarizes the report and presents recommendations for further work. In particular, the recommendation to use data collected at the ground monitor stations to validate the models of Chapter 2 and Appendices A and B is explained.

---

*No other changes have been made to the TRACOR 7620 navigation algorithm, and TRACOR, Inc. did not have the opportunity to optimize the design for the differential Omega application.

2. ANALYTICAL FORMULATION

The differential Omega experiment will involve testing the TRACOR 7620 navigation set in two modes: the differential mode when monitor corrections are available, and the stand-alone Omega mode when corrections are not available. In both modes, the navigation set must perform two functions: process phase measurements to obtain an Omega position fix, and integrate additional sensors (viz. true airspeed and heading) to provide continuous navigation displays.

Omega position fix quality is evaluated using an error model for Omega signal propagation uncertainties as well as for receiver errors. The Omega propagation model described herein is a statistical model derived from measurements made on the Omega Navigation System at several fixed sites throughout the world (Ref. 2). The data used to calibrate the model were all obtained for the lowest Omega frequency, 10.2 kHz.

Application of this model to this differential Omega experiment relies on two key assumptions:

- The same model structure can be used to describe Omega errors at 13.6 kHz
- The parameter values obtained from the worldwide data base are appropriate for the Alaska/Yukon region.

Parameter values obtained from Ref. 2 were chosen as the "nominal values" in the analysis, and an analysis was performed to evaluate the sensitivity of the performance predictions to variations in the parameter values. (The sensitivity analysis is

presented in Chapter 3 in the form of curves in which a wide range of variation about the nominal parameter value is evaluated.)

Evaluation of the TRACOR 7620 as a navigation set involves simulating the performance of the navigation algorithm along specific flight profiles in the Alaska/Yukon region using appropriate environmental parameters for that region. The simulations are performed using computer programs previously developed by TASC for the TRACOR 7620 navigation set (Ref. 7). These programs model the TRACOR 7620 from the output of the receiver phase trackers to the output of the navigation processor.

The relationship between the various analytical formulations and the significance attached to the results are described in Section 2.1. The statistical Omega phase error model is summarized in Section 2.2. (The model is described in more detail in Appendix A and a theoretical discussion of the most significant model parameter, the correlation coefficient between errors on both frequencies from the same Omega transmitting station, is presented in Appendix B.) Section 2.3 contains a brief description of the TRACOR 7620 navigation algorithm.

2.1 METHODOLOGY

The method used to evaluate the performance of the differential Omega experiment in the Alaska/Yukon region, using the TRACOR 7620, is summarized in Fig. 3. Two analysis techniques (statistical and direct simulation) are used to analyze the effects of three error sources: Omega phase error, wind error, and instrument error. The contribution of each of these error sources to navigation error in the TRACOR 7620 navigation

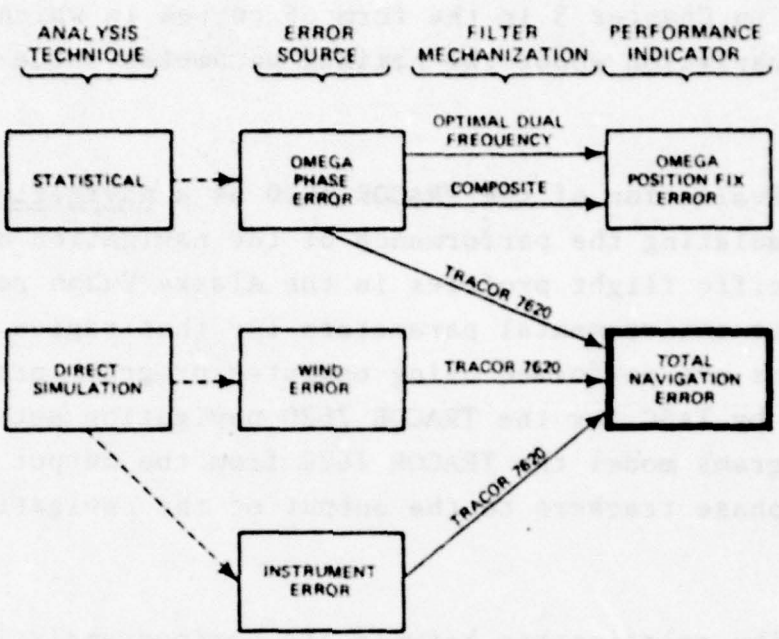

Figure 3 Overview of Analysis Methodology

filter is determined. The combined contributions of the individual error sources provide a performance estimate of the accuracy of the TRACOR 7620 navigation display. In addition, accuracy obtainable from a single Omega position fix is evaluated using two techniques: optimal (least-squares) use of Omega phase information on two frequencies defines the best position fixing available to a navigation set with a similar hardware configuration, and use of the specific TRACOR 7620 composite Omega mechanization describes the quality of the input to the navigation algorithm.

Wind errors are observed by the TRACOR 7620 navigation algorithm through the Omega position fixes. Changes in groundspeed and direction result from shifts in the wind, since the aircraft normally attempts to fly at constant airspeed. A direct simulation of the effect of winds is used to assess the impact of wind error. The computer programs used in the analysis were previously developed by TASC for the TRACOR 7620 navi-

gation set (Ref. 7). Satisfactory filter response to a worst-case wind error condition is used to establish the suitability of the filter for this application. Additional information is supplied to the navigation filter by a heading reference and an airspeed indicator. Reliable error models for these instruments were not available for this study, and the contribution of nominal errors from these instruments to navigation error is not considered. However, the impact of instrument failure on navigation error is studied by direct simulation techniques. The combined effect of Omega phase error, wind error, and instrument failure on the TRACOR 7620 navigation filter provides an estimate of the accuracy of the total navigation display in the aircraft. Since nominal instrument errors are not considered, accuracy predictions for the total navigation display under nominal conditions apply only to a navigator with perfect heading and airspeed information.

To evaluate the full potential of the differential Omega concept, an analysis is performed to determine the accuracy achievable from usage of phase information in a single Omega position fix. A lower bound on Omega position fix accuracy is provided by optimal (least-squares) processing of the dual-frequency phase information from four stations. A second measure of Omega position fix accuracy is provided by the composite mechanization used as an input to the TRACOR 7620 navigation filter. The composite mechanization evaluation does not directly measure the performance of any part of the TRACOR 7620 filter; however, it does provide a lower bound on the Omega position fix accuracy used as an input to the filter. The performance of these two estimators (optimal and composite) serves to establish the performance obtainable with differential Omega operating as a simple display of instantaneous position without considering the navigation function. Although the potential benefits associated with phase measurement averaging are not realized, the errors and response characteristics asso-

ciated with a specific navigation mechanization are also eliminated. Omega position fix evaluation also provides a convenient mechanism to evaluate the sensitivity of performance to changes in parameters of the Omega phase error model.

2.2 PHASE ERROR MODEL

Navigation error, $\underline{\Delta x}$, is defined as the vector difference between the receiver-indicated position, $\underline{x}_i$, and the true position, $\underline{x}_t$, where:

$$\underline{\Delta x} = \underline{x}_t - \underline{x}_i \tag{1}$$

It is convenient to express navigation error in terms of north and east position error components on the surface of the earth (ΔN and ΔE, respectively). If the position deviations are small relative to the range to an Omega transmitting station, the equivalent phase deviation associated with the position deviation is a simple function of the bearing angle to the station. Omega phase measurements also include errors caused by propagation anomalies and receiver measurement errors. The resulting linearized scalar expression for the measured phase deviation caused by navigation error and by propagation and receiver errors is

$$\Delta\phi_{ij} = \frac{1}{\lambda_j} \cos \Psi_i \, \Delta N + \frac{1}{\lambda_j} \sin \Psi_i \, \Delta E + \delta\phi_{ij} \tag{2}$$

where

$\Delta\phi_{ij}$ is the measured phase deviation from station i on frequency j

λ_j is the wavelength of the signal with frequency j

Ψ_i is the bearing angle to station i

$\delta\phi_{ij}$ is the phase error from station i on frequency j caused by propagation error and receiver error.

It is convenient to write Eq. 2 in matrix form by defining a vector of phase measurement deviations, $\underline{\Delta\phi}$, which includes as components all of the eight available signals:

$$\underline{\Delta\phi} = H\,\underline{\Delta x} + \underline{\delta\phi} \qquad (3)$$

where

H is the measurement geometry matrix

$\underline{\Delta x}$ is the vector of north and east position errors

$\underline{\delta\phi}$ is the vector of phase errors.

When signal phase measurements from more than three separate transmitting stations are made, redundant information is available which can be used to reduce navigation error. The impact of Omega phase error on navigation error depends on the manner in which the navigation set uses the phase measurements. As previously noted, two techniques for using phase information are evaluated:

- Optimal - A minimum-variance ("least-squares") estimate of position based on all available phase measurements
- Composite Mechanization - A suboptimal estimate of position based on the specific combination of phase measurements implemented at the input to the TRACOR 7620.

Note that the optimal formulation will always provide the smaller error (under nominal conditions); a suboptimal technique

such as the TRACOR 7620 mechanization, however, may be simpler to implement and may possibly exhibit less sensitivity to modeling errors.

2.2.1 Optimal Processing of Phase Measurements

The minimum variance estimate, $\underline{\hat{\Delta x}}$, of the position deviations is (*Ref. 10*)

$$\underline{\hat{\Delta x}} = (H^T R^{-1} H)^{-1} H^T R^{-1} \underline{\Delta\phi} \tag{4}$$

where

$$R = E[\underline{\delta\phi}\ \underline{\delta\phi}^T]$$

$E[\cdot]$ denotes the expected value operator.

The covariance of the error in the estimate $\underline{\hat{\Delta x}}$ is

$$P = (H^T R^{-1} H)^{-1} \tag{5}$$

where

$$P = E\{(\underline{\hat{\Delta x}} - \underline{\Delta x})(\underline{\hat{\Delta x}} - \underline{\Delta x})^T\}$$

A statistical model for $\delta\phi_{ij}$ is required to form R. Details of the model for $\delta\phi_{ij}$ are presented in Appendix A. A summary of the salient characteristics of the model is presented in Table 2.

2.2.2 Composite Mechanization

In the TRACOR 7620 navigation set, eight Omega phases are combined to form three composite phase measurements with the following general form:

TABLE 2

SUMMARY OF COMPONENTS OF NOMINAL PHASE ERROR COVARIANCE MATRIX MODEL

T-3436

RANDOM PROPAGATION ERROR MODEL

$$E[\delta\phi^r_{i,10.2}(\underline{x}_2,t_2)\delta\phi^r_{i,10.2}(\underline{x}_1,t_1)] = \exp\left[-\frac{|\underline{x}_2 - \underline{x}_1|}{d}\right]\left\{\sigma_1^2 \exp\left[\frac{|t_2 - t_1|}{\tau_1}\right] + \sigma_2^2 + \sigma_3^2 \cos\left(\frac{2\pi}{T_3}|t_2 - t_1|\right) + \sigma_4^2 \cos\left(\frac{2\pi}{T_4}|t_2 - t_1|\right)\right\}$$

$d = 1500$ nm $\quad \sigma_1^2 = 9.83$ cec^2 $\quad |t_2 - t_1|$ = average monitor update delay = 3 min

$\tau_1 = 0.943$ hr $\quad \sigma_2^2 = 17.8$ cec^2

$T_3 = 12$ hr $\quad \sigma_3^2 = 8.13$ cec^2

$T_4 = 8$ hr $\quad \sigma_4^2 = 1.98$ cec^2

$$E[\delta\phi^r_{i,13.6}(\underline{x}_2,t_2)\delta\phi^r_{i,13.6}(\underline{x}_1,t_1)] = W^2\, E[\delta\phi^r_{i,10.2}(\underline{x}_2,t_2)\,\delta\phi^r_{i,10.2}(\underline{x}_1,t_1)];\ W = 1$$

$$E[\delta\phi^r_{ij}(\underline{x}_2,t_2)\delta\phi^r_{ik}(\underline{x}_1,t_1)] = \rho W\, E[\delta\phi^r_{i,10.2}(\underline{x}_2,t_2)\delta\phi^r_{i,10.2}(\underline{x}_1,t_1)],\ \rho = 0.5$$

RECEIVER ERROR MODEL

$$E[\delta\phi^v_{ij}(\underline{x},t)]^2 = \sigma_v^2,\ \sigma_v = 0.5 \text{ cec}$$

$$\phi_{ij,c} = a(\phi_{i,13.6} - \phi_{j,13.6}) - b(\phi_{i,10.2} - \phi_{j,10.2}) \qquad (6)$$

where

$\phi_{ij,c}$ is the composite phase from stations i and j

$\phi_{i,13.6}$ is the phase from station i at 13.6 kHz

$\phi_{j,10.2}$ is the phase from station j at 10.2 kHz

a,b are constants (a = 15/8 and b = 3/2 for the TRACOR 7620).

The relation between composite phase deviation and position error for this set is (from Eqs. 2 and 6)

$$\Delta\phi_{ij,c} = \frac{1}{\lambda_c}(\cos\Psi_i - \cos\Psi_j)\Delta N + \frac{1}{\lambda_c}(\sin\Psi_i - \sin\Psi_j)\Delta E + \delta\phi_{ij,c} \tag{7}$$

where λ_c is the composite wavelength given by $\left(\frac{a}{\lambda_{13.6}} + \frac{b}{\lambda_{10.2}}\right)^{-1}$

If the scalar composite phase deviations are combined to form a vector of composite phases (denoted by $\underline{\Delta\phi}_c$), the derivation of Eqs. 3 - 5 can be applied to the TRACOR 7620 processing.

2.3 TRACOR 7620 NAVIGATION FILTER

The TRACOR implementation of the Omega navigation algorithm is a suboptimal Kalman-like filter (Ref. 17). It contains a four-state dynamic model that allows position prediction and correction. This section presents a derivation of an error model for this algorithm and describes some of its characteristics.

2.3.1 TRACOR Algorithm

The TRACOR algorithm has two sections: a dead-reckoning section, which uses airspeed and heading information, and an update section that processes Omega measurements.

Dead-Reckoning - The dead-reckoning section performs a rectangular integration of a four-element state vector every 1.25 sec. The filter states are latitude and longitude, in radians, and latitude and longitude wind rate, in radians per second:

$$\hat{\underline{x}} = [\hat{LAT},\ \hat{LON},\ \hat{WIND}_N,\ \hat{WIND}_E]^T \tag{8}$$

The dead-reckoning equation is:

$$\hat{\underline{x}}(kT) = \begin{bmatrix} 1 & 0 & 1.25 & 0 \\ 0 & 1 & 0 & 1.25 \\ 0 & 0 & 1 & 0 \\ 0 & 0 & 0 & 1 \end{bmatrix} \hat{\underline{x}}(kT-T) + 1.25 \begin{bmatrix} \cos TH \\ \dfrac{\sin TH}{\cos LAT} \\ 0 \\ 0 \end{bmatrix} \frac{TAS}{3600R_e} \tag{9}$$

where

TH is the true heading

TAS is the true airspeed (kt)

R_e is the radius of the earth (nm)

Omega Updates - Every 10 sec, the algorithm processes a set of Omega measurements and applies a correction to the current state estimate:

$$\hat{\underline{x}}(kT^+) = \hat{\underline{x}}(kT^-) + K[\underline{z} - \underline{\phi}_c(\hat{\underline{x}}(kT^-))] \tag{10}$$

where $\underline{z}$ is the vector of observed phases and $\underline{\phi}_c(\hat{\underline{x}})$ is the vector of estimated composite phases, as a function of estimated position.

The filter gain matrix K is variable and depends on estimated position:

$$K = P_f\ H(\hat{\underline{x}})\ R_f^{-1} \tag{11}$$

P_f and R_f^{-1} are fixed, while H depends on station geometry. The TRACOR 7620 navigation filter does not update the matrix P_f.

2.3.2 TRACOR Error Model

From Appendix C, the position and wind errors in the TRACOR 7620 state-vector estimates are given by

$$\underline{\Delta x}(kT) = [I-KH]\,[\Phi\,\underline{\Delta x}(kT-T) + L(\underline{w}(kT-T) - \underline{w}(kT)) + G\underline{v}_m(kT)] + K\underline{v}(kT) \qquad (12)$$

where

- Φ is the state transition matrix
- G is the noise weighting matrix
- L is the control weighting matrix
- $\underline{w}$ is the wind vector
- $\underline{v}_m$ is the instrument error vector
- $\underline{v}$ is the Omega phase measurement error vector.

Equation 12 is used to evaluate the steady-state response of the TRACOR 7620 navigation filter to these error sources.

3. PERFORMANCE PREDICTIONS

3.1 INTRODUCTION

Differential Omega is under consideration as a non-precision approach aid and as an enroute aid between airports. In this chapter, the model for differential Omega phase error presented in Appendix A and the TRACOR 7620 navigation set implementation described in Appendix C are used to predict navigation performance for both applications. In Section 3.2, the expected nominal position error near an airport is presented along with the performance sensitivity to assumed operating conditions and to the assumed model parameters. The use of differential corrections in the enroute mode is analyzed in Section 3.3.

3.2 USE AS A NON-PRECISION APPROACH AID

3.2.1 Nominal Performance

The expected performance of a differential Omega navigation set on an approach to Inuvik, 2 nm away, is presented in Table 3. Because of the high sensitivity of the composite mechanization to the correlation between frequencies, ρ, (see Section 3.2.3) results are presented for a worst-case nominal correlation, $\rho=0.5$, and also for $\rho=0.9$. In addition, performance predictions for a single-frequency mechanization as well as performance predictions with no differential corrections are included for comparison. Along- and cross-track position error estimates are provided for an approach to Inuvik at a geodetic bearing of 90 deg. The along- and cross-track estimates in Table 3 are combined to give radial position error in

TABLE 3

RMS ALONG-TRACK/CROSS-TRACK POSITION ERROR FOR BASELINE CONDITIONS

(2 nm FROM INUVIK)

T-3437

CATEGORY	DIFFERENTIAL SYSTEM POSITION ERROR (nm)			NON-DIFFERENTIAL SYSTEM POSITION ERROR (nm)		
	PROPAGATION	RECEIVER	TOTAL	PROPAGATION	RECEIVER	TOTAL
Position-Fix						
Composite mechanization, ρ=0.5 (nominal)	0.26/0.18	0.18/0.12	0.32/0.22	1.60/1.04	0.18/0.12	1.61/1.05
Composite mechanization, ρ=0.9	0.13/0.087	0.18/0.12	0.22/0.15	0.78/0.51	0.18/0.12	0.80/0.52
13.6 kHz only	0.12/0.078	0.057/0.037	0.13/0.086	0.70/0.45	0.057/0.037	0.70/0.45
Optimal, ρ=0.5 (nominal)	0.12/0.075	0.045/0.029	0.13/0.080	0.67/0.43	0.045/0.029	0.67/0.43
Optimal, ρ=0.9	0.11/0.074	0.045/0.029	0.12/0.079	0.66/0.43	0.045/0.029	0.66/0.43
TRACOR 7620 Navigation Filter						
ρ=0.5 (nominal)	0.23/0.22	0.060/0.11	0.24/0.25	1.3/1.2	0.060/0.11	1.3/1.2
ρ=0.9	0.11/0.11	0.060/0.11	0.13/0.16	0.62/0.58	0.060/0.11	0.62/0.59

TABLE 3

RMS ALONG-TRACK/CROSS-TRACK POSITION ERROR FOR BASELINE CONDITIONS

(2 nm FROM INUVIK)

T-3437

CATEGORY	DIFFERENTIAL SYSTEM POSITION ERROR (nm)			NON-DIFFERENTIAL SYSTEM POSITION ERROR (nm)		
	PROPAGATION	RECEIVER	TOTAL	PROPAGATION	RECEIVER	TOTAL
Position-Fix						
Composite mechanization, ρ=0.5 (nominal)	0.26/0.18	0.18/0.12	0.32/0.22	1.60/1.04	0.18/0.12	1.61/1.05
Composite mechanization, ρ=0.9	0.13/0.087	0.18/0.12	0.22/0.15	0.78/0.51	0.18/0.12	0.80/0.52
13.6 kHz only	0.12/0.078	0.057/0.037	0.13/0.086	0.70/0.45	0.057/0.037	0.70/0.45
Optimal, ρ=0.5 (nominal)	0.12/0.075	0.045/0.029	0.13/0.080	0.67/0.43	0.045/0.029	0.67/0.43
Optimal, ρ=0.9	0.11/0.074	0.045/0.029	0.12/0.079	0.66/0.43	0.045/0.029	0.66/0.43
TRACOR 7620 Navigation Filter						
ρ=0.5 (nominal)	0.23/0.22	0.060/0.11	0.24/0.25	1.3/1.2	0.060/0.11	1.3/1.2
ρ=0.9	0.11/0.11	0.060/0.11	0.13/0.16	0.62/0.58	0.060/0.11	0.62/0.59

Table 4. Radial position error is used as the measure of performance throughout the remainder of this chapter.

Results of the position-fix error analysis show:

- Optimal position-fix performance is not sensitive to the correlation coefficient ρ. The total error of 0.15 nm is produced almost entirely by propagation prediction errors
- Nominal composite mechanization position-fix performance for $\rho=0.9$ has a position error due to propagation errors which is nearly optimal, but a relatively large contribution of receiver error causes performance to be significantly inferior to the optimal position-fix result
- Processing phase measurements from only 13.6 kHz signals provides nearly optimal position-fix performance which is significantly superior to the composite-frequency mechanization
- Differential corrections from a monitor are effective in reducing position error in all cases.

3.2.2 Sensitivity to Operating Conditions

In this section, the impact on navigation accuracy of changes in the following operating conditions is presented:

- Airport location
- Vehicle maneuvers
- Station outage
- Loss of instruments
- Monitor update delay (signal averaging time).

TABLE 4

RMS RADIAL POSITION ERROR FOR BASELINE CONDITIONS

(2 nm FROM INUVIK)

T-3438

CATEGORY	DIFFERENTIAL SYSTEM POSITION ERROR (nm)			NON-DIFFERENTIAL SYSTEM POSITION ERROR (nm)		
	PROPAGATION	RECEIVER	TOTAL	PROPAGATION	RECEIVER	TOTAL
Position-Fix						
Composite mechanization, ρ=0.5 (nominal)	0.33	0.22	0.40	1.91	0.22	1.92
Composite mechanization, ρ=0.9	0.16	0.22	0.27	0.93	0.22	0.96
13.6 kHz only	0.14	0.068	0.16	0.83	0.068	0.83
Optimal, ρ=0.5 (nominal)	0.14	0.054	0.15	0.80	0.054	0.80
Optimal, ρ=0.9	0.14	0.054	0.15	0.79	0.054	0.79
TRACOR 7620 Navigation Filter						
ρ=0.5 (nominal)	0.32	0.093	0.33	1.7	0.093	1.7
ρ=0.9	0.16	0.093	0.18	0.85	0.093	0.86

Sensitivity to Airport Location - Since the estimation gain matrix depends on station receiver geometry, position error response will change from one location to another. In particular, response improves as the vectors to the stations become more nearly perpendicular (Ref. 7). Nevertheless, station geometry does not vary greatly in the region of interest. (See Fig. 4. Arrows represent range and bearing to transmitting stations. MM denotes megameter.) Geometry appears to be the best at Fairbanks and the worst at Inuvik.

Table 5 shows the effect of geometry on the statistical performance of the position-fix and navigation filter position estimates. Performance at locations near the three different airports under consideration is nearly the same, but is generally best at Fairbanks and worst at Inuvik.

To test the effect of these different geometries on the TRACOR 7620 navigation filter dynamics, simulated error histories were generated for areas near Fairbanks and Inuvik.

TABLE 3.2-3
RMS RADIAL POSITION ERROR FOR DIFFERENT AIRPORTS
(2 nm FROM AIRPORT)

CATEGORY \ AIRPORT	RMS RADIAL POSITION ERROR (nm)		
	INUVIK	FAIRBANKS	DEADHORSE
Position-fix			
Composite mechanization (ρ=0.5)	0.40	0.35	0.36
Optimal (ρ=0.5)	0.15	0.13	0.14
TRACOR 7620			
Navigation Filter	0.33	0.34	0.34

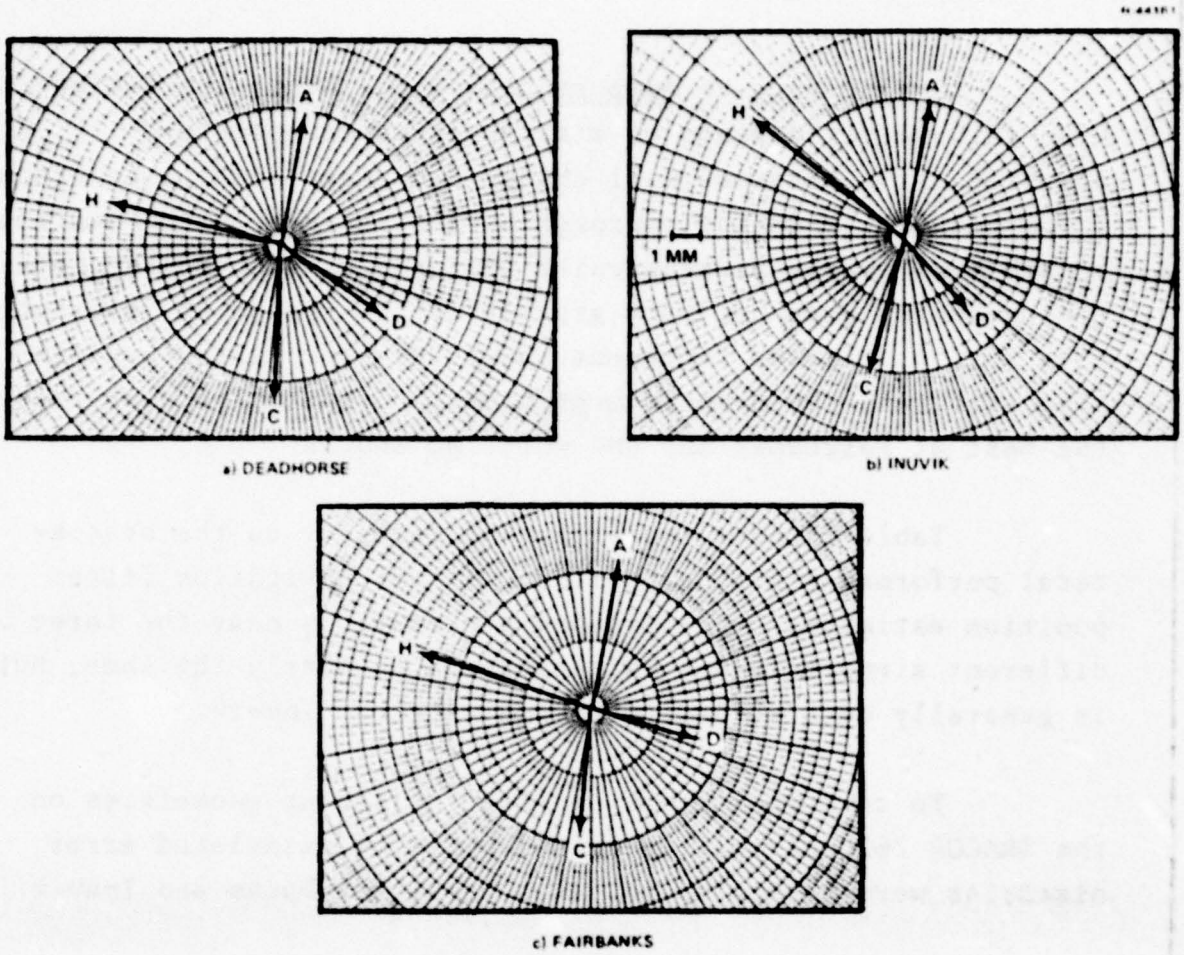

Figure 4 Omega Geometry at Selected Sites

Only three Omega signals were simulated in order to accentuate the effects of geometry. All other conditions were held constant:

- Airpseed: 250 kt
- Initial track: 180°
- Wind steps from zero to 10 kt after 2 min into flight
- Aircraft turns clockwise through 270° (from 0°) at 3°/sec after 10 min into flight
- Signals from transmitting stations C, D, H assumed to be available

- Noise-free reception and error-free differential corrections available
- Continuous true airspeed and stabilized heading data available.

Figure 5 depicts the simulation results for trajectories near Fairbanks and Inuvik. Maximum position error for the Inuvik simulation is approximately 10% greater than the maximum position error for the Fairbanks simulation. Error dynamics are essentially the same at both locations.

These results demonstrate that Omega geometry has very little effect on performance over the region of interest. However, performance near Inuvik may be taken as worst-case.

Maneuver Sensitivity - Since the TRACOR navigation filter depends on a 1.25 sec rectangular integrator, it may be possible for a maneuver to create unacceptably large position errors. A simulated error history was generated to determine the sensitivity of position error to a maximum procedure turn for the following conditions:

- Initial position: 68°N, 134°W
- Airspeed: 250 kt
- Initial track: 180°
- Aircraft turns clockwise through 270° at 3°/sec after 60 min into flight
- Signals from transmitting stations A, C, D, H assumed to be available
- Noise-free reception and error-free differential corrections available
- Continuous true airspeed and stabilized heading data available.

Results of this simulation are shown in Fig. 6.

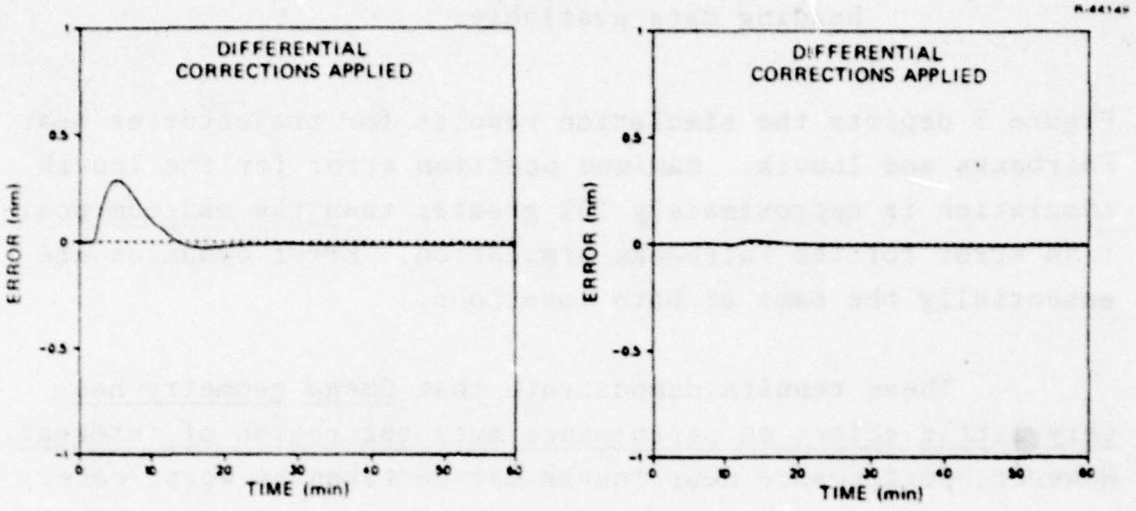

a) North Position Error, Inuvik

b) East Position Error, Inuvik

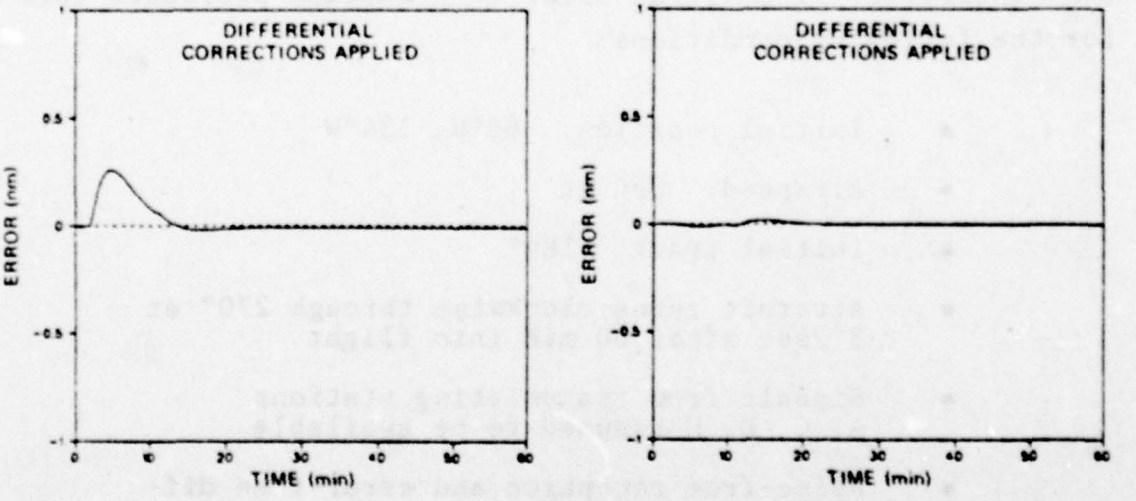

c) North Position Error, Fairbanks

d) East Position Error, Fairbanks

Figure 5 Effect of Airport Location on TRACOR 7620 Navigation Performance

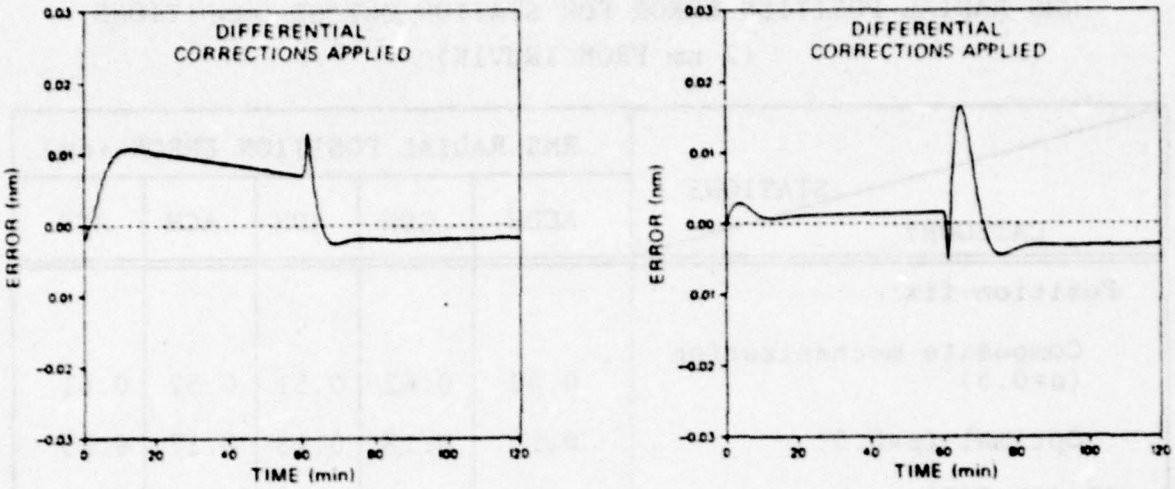

a) North Position Error

b) East Position Error

Figure 6 Effect of Maneuvers on TRACOR 7620 Navigation Performance

Initially, small position errors occur due to numerical errors in simulation initialization. At the start of the turn, a sharp transient appears. It reaches a maximum radial position error of approximately 0.02 nm and quickly decays. Athough a maneuver introduces some position error, the resulting maximum radial error is not likely to exceed 0.02 nm. The maneuver-induced error decays quickly, and system stability is not compromised by maneuvers.

Sensitivity to Station Outage - In the Alaska/Yukon region, signals for Omega transmitting stations A, C, D, and H can generally be received. In the event of signal loss from one of these stations, performance degrades to the levels shown in Table 6. Performance degradation is largest for loss of signals from either station A or H.

TABLE 6

RMS RADIAL POSITION ERROR FOR STATION OUTAGE CONDITIONS

(2 nm FROM INUVIK)

CATEGORY \ STATIONS	RMS RADIAL POSITION ERROR (nm)				
	ACDH	CDH	ADH	ACH	ACD
Position-fix					
Composite mechanization (ρ=0.5)	0.40	0.62	0.51	0.52	0.61
Optimal (ρ=0.5)	0.15	0.18	0.18	0.17	0.19
TRACOR 7620					
Navigation filter	0.33	0.45	0.39	0.45	0.39

To examine the effect of the loss of one station on the position error dynamics of the TRACOR 7620 filter, two simulations were run. Figures 5a and 5b present results for a receiver near Inuvik when signals from transmitting stations C, D, and H are received. In Fig. 7 results correspond to signals from stations A, C, D and H being used. Other simulation parameters are:

- Initial position: 68°N, 134°W
- Airspeed: 250 kt
- Initial track: 180°
- North wind steps from zero to 10 kt after 2 min into flight
- Aircraft turns clockwise through 270° at 3°/sec after 20 min into flight
- Noise-free reception and perfect differential corrections available
- Continuous true airspeed and stabilized heading data available.

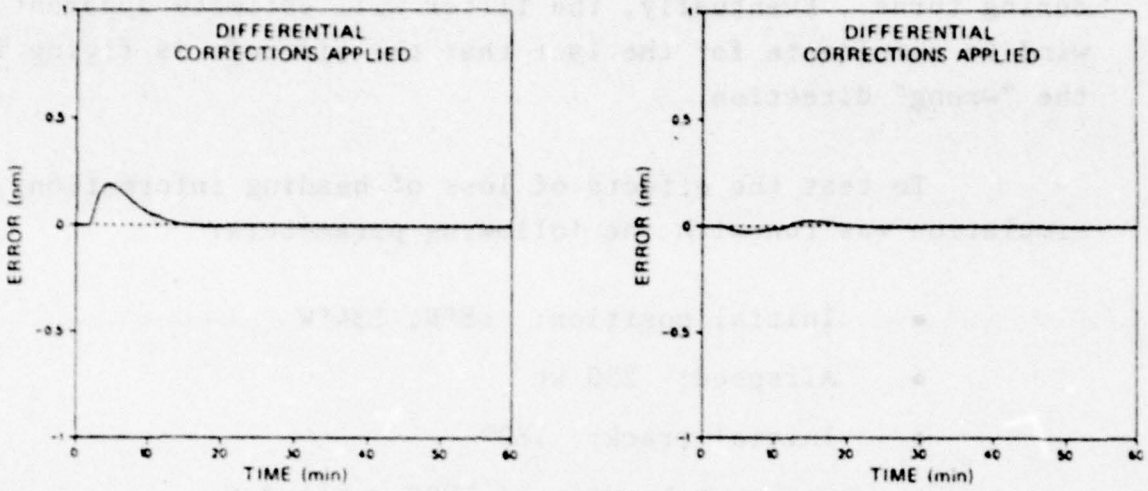

a) North Position Error b) East Position Error

Figure 7 Effect of Signal Availability on TRACOR 7620 Navigation Performance

The maximum radial position error increases 50% with this loss of station A, from approximately 0.2 nm with signals from four stations received, to 0.3 nm with signals from three stations received. Also note that the maximum radial error occurs at a slightly later time in the three-station case than in the four-station case.

Sensitivity to Loss of Instruments - The TRACOR 7620 position dead-reckoner requires airspeed and heading information. If these inputs are lost, position errors will increase. Loss of heading and airspeed information are simulated separately, as described below.

First, assume that true heading data are lost and the filter continues to use the last known heading. As long as the aircraft continues to fly in a straight line, no errors occur. However, large transient position errors are expected

during turns. Eventually, the filter will estimate apparent wind to compensate for the fact that the aircraft is flying in the "wrong" direction.

To test the effects of loss of heading information, a simulation was run with the following parameters:

- Initial position: 68°N, 134°W
- Airspeed: 250 kt
- Initial track: 180°
- Constant heading of 180° applied to filter
- Aircraft turns clockwise through 270° at 3°/sec after 10 min into flight
- Signals from transmitting stations A, C, D, and H assumed to be available
- Noise-free reception and error-free monitor corrections assumed
- Continuous true airspeed data available.

As Fig. 8 shows, large transient errors occur and reach a maximum radial position error of approximately 8.5 nm. This deterministic effect is sufficiently large to dominate the random errors associated with Omega phase measurements. Recovery of TRACOR 7620 filter takes more than 20 min since measurements must propagate through two state variables, wind and position. Also note that north and east wind estimates reach steady-state values of 250 kt. This would be sufficient wind to move the aircraft east at the known true airspeed even if the true heading were south, as the dead-reckoner assumes.

Now, suppose that airspeed information is lost and the filter continues to use the last known value. Z-transform analysis (see Appendix C) indicates that long-term position

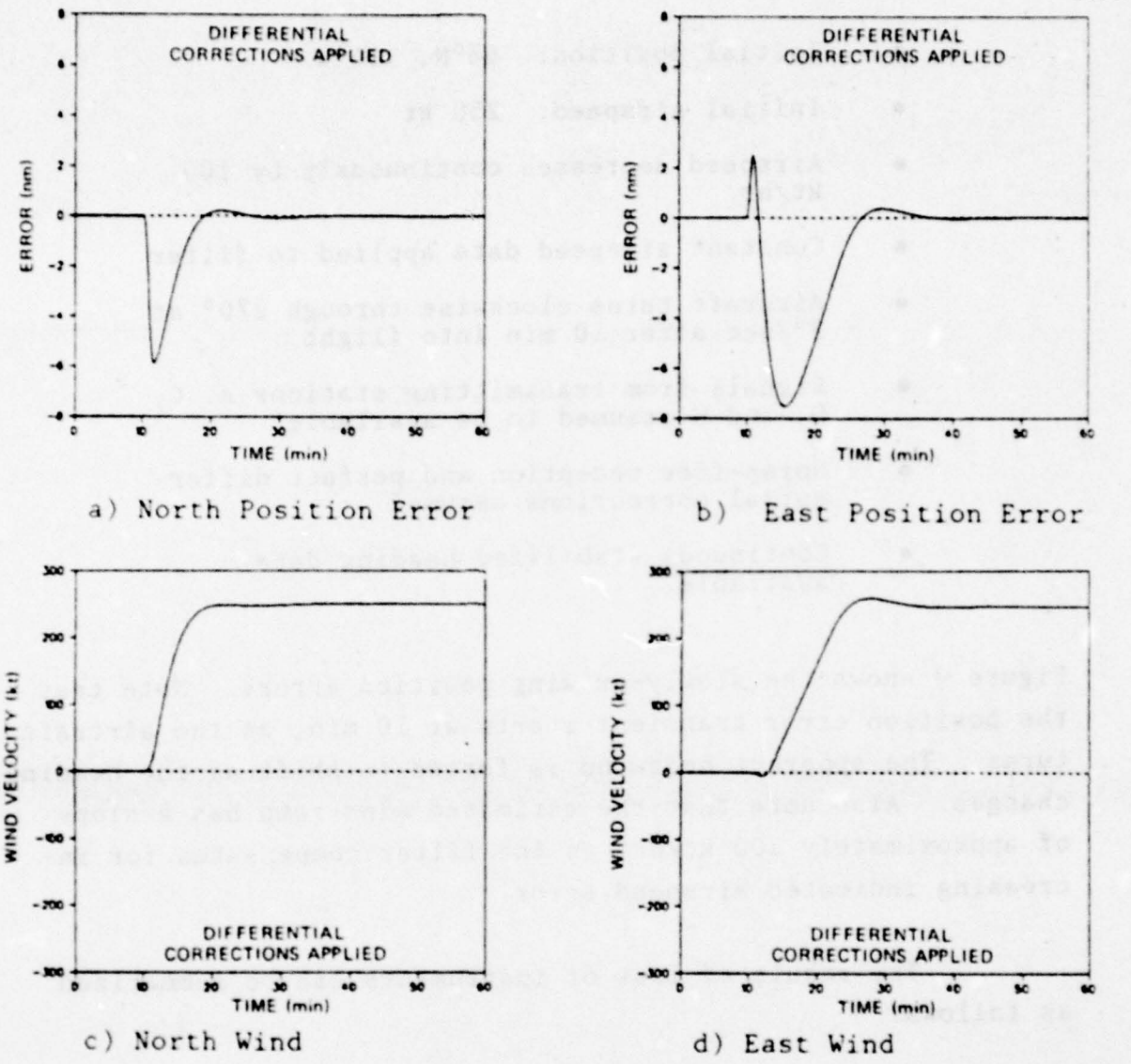

Figure 8 Effect of Loss of Heading Data on TRACOR 7620 Navigation Performance

errors due to increasing airspeed errors should be slowly-growing but unbounded. Wind estimates should compensate for most of the airspeed error. To test the effect of loss of airspeed data on TRACOR 7620 position error, a simulation was run with these parameters:

- Initial position: 68°N, 134°W
- Initial airspeed: 250 kt
- Airspeed decreases continuously by 100 kt/hr
- Constant airspeed data applied to filter
- Aircraft turns clockwise through 270° at 3°/sec after 10 min into flight
- Signals from transmitting stations A, C, D, and H assumed to be available
- Noise-free reception and perfect differential corrections assumed
- Continuous stabilized heading data available.

Figure 9 shows the slowly-growing position errors. Note that the position error transient starts at 10 min, as the aircraft turns. The apparent headwind is forced to shift as the heading changes. Also note that the estimated wind ramp has a slope of approximately 100 kt/hr, as the filter compensates for increasing indicated airspeed error.

The result of loss of instruments can be summarized as follows:

- Loss of stabilized heading data results in large position error transients after each maneuver that eventually damp to zero
- Loss of airspeed information results in relatively slowly-growing position errors which eventually become unbounded.

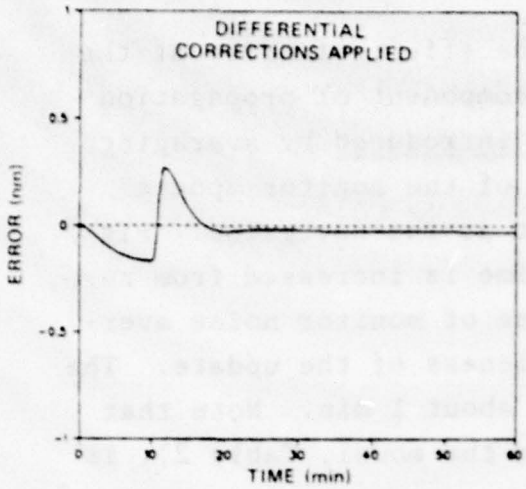

a) North Position Error

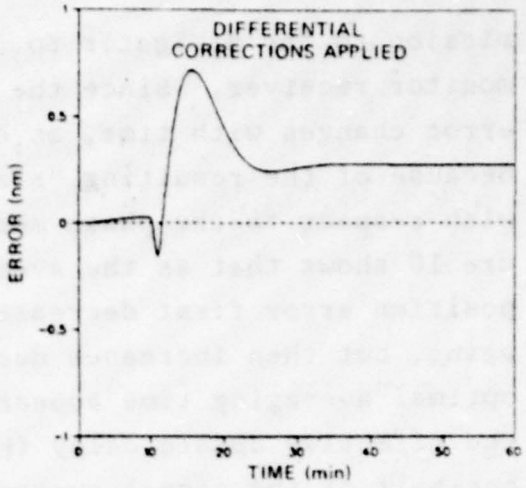

b) East Position Error

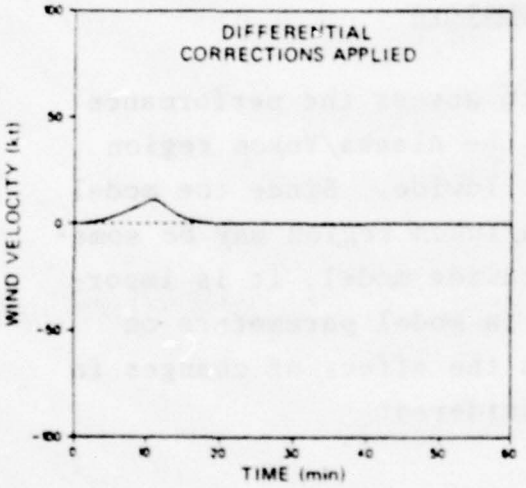

c) North Wind

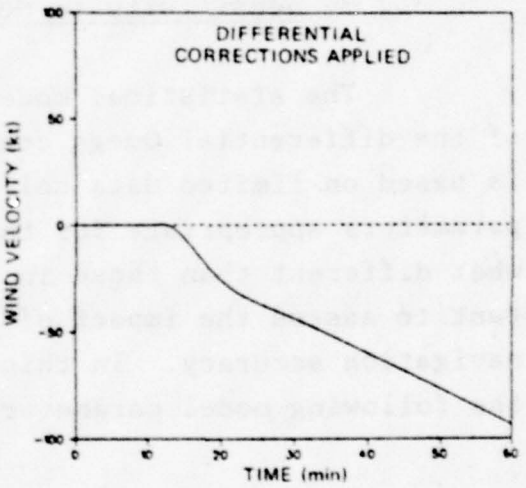

d) East Wind

Figure 9 Effect of Loss of Airspeed Data on TRACOR 7620 Navigation Performance

Update delay - Under nominal conditions, phase measurements at the monitor are averaged* for 6 min before trans-

*Averaging is a consequence of the narrow tracking bandwidth in the TRACOR 599R monitor receiver. The filters being used by Transport Canada for this experiment have an equivalent averaging time of approximately 5 min.

mission to the navigator to reduce the effect of noise at the monitor receiver. Since the random component of propagation error changes with time, an error is introduced by averaging because of the resulting "staleness" of the monitor update with respect to the phase measurement at the navigator. Figure 10 shows that as the averaging time is increased from zero, position error first decreases because of monitor noise averaging, but then increases due to staleness of the update. The optimal averaging time appears to be about 1 min. Note that the effective update delay ($|t_2-t_1|$ in the model, Table 2), is one-half of the signal averaging time.

3.2.3 Sensitivity to Model Parameters

The statistical model used to assess the performance of the differential Omega concept in the Alaska/Yukon region is based on limited data collected worldwide. Since the model parameters appropriate for the Alaska/Yukon region may be somewhat different than those in the worldwide model, it is important to assess the impact of changes in model parameters on navigation accuracy. In this section the effect of changes in the following model parameters is considered:

- Correlation coefficient between frequencies (ρ)
- Correlation distance (d)
- Correlation time (τ_1)
- Standard deviation of random phase error ($\sqrt{\sigma_1^2 + \sigma_2^2 + \sigma_3^2 + \sigma_4^2}$)
- Receiver error.

Correlation coefficient - As shown in Fig. 11, an increase in the frequency cross-correlation coefficient above

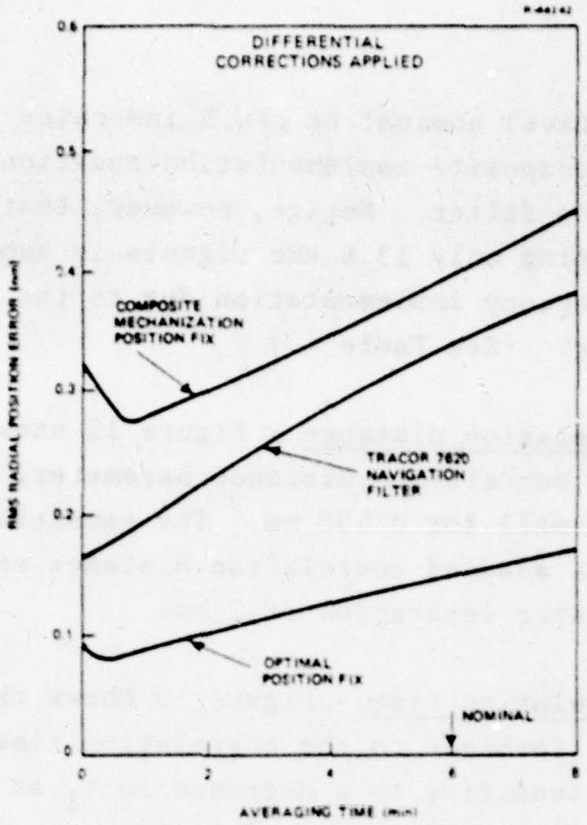

Figure 10 Sensitivity of RMS Radial Position Error to Signal Averaging Time at the Monitor (2 nm from Inuvik)

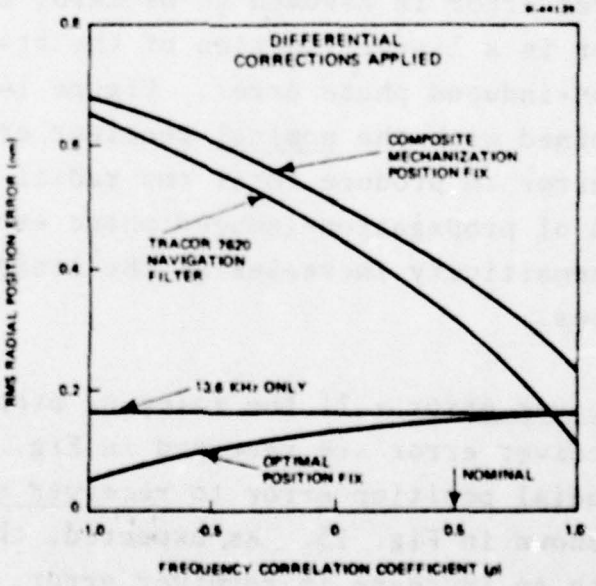

Figure 11 Sensitivity of RMS Radial Position Error to 10.2 kHz/13.6 kHz Frequency Correlation Coefficient, ρ (2 nm from Inuvik)

the (conservative) nominal of ρ=0.5 indicates improved performance for the composite implementation position-fix and TRACOR 7620 navigation filter. Notice, however, that even when ρ=1, performance using only 13.6 kHz signals is superior to the composite-frequency implementation due to the contribution of receiver error. (See Table 4.)

Correlation distance - Figure 12 shows that sensitivity to the correlation distance parameter, d, in the model is extremely small for d>500 nm. The sensitivity increases rapidly as the assumed correlation distance approaches the monitor-navigator separation of 2 nm.

Correlation time - Figure 13 shows the sensitivity of navigation performance to the correlation time, τ_1. Performance is very sensitive to a decrease in τ_1 as it approaches the nominal update delay time of 3 min.

Standard deviation of propagation-induced phase error - If the receiver error is assumed to be zero, then rms radial position error is a linear function of the standard deviation of propagation-induced phase error. Figure 14 shows this linear function combined with the nominal receiver error contribution to position error to produce total rms radial position error as a function of propagation-induced phase error standard deviation. The sensitivity increases as the residual propagation error increases.

Receiver error - If the roles of propagation-induced error and receiver error are reversed in Fig. 14, the sensitivity of rms radial position error to receiver error is obtained. Results are shown in Fig. 15. As expected, the position error increases with an increase in receiver error.

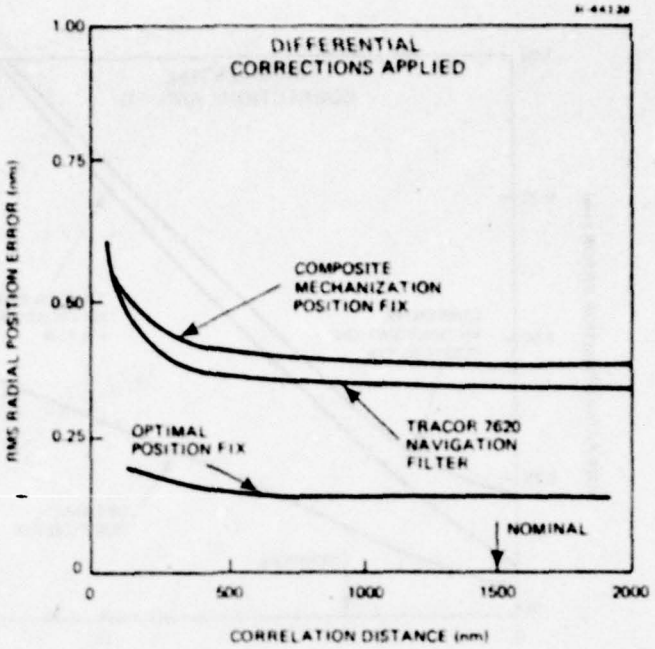

Figure 12 Sensitivity of RMS Radial Position Error to Correlation Distance, d (2 nm from Inuvik)

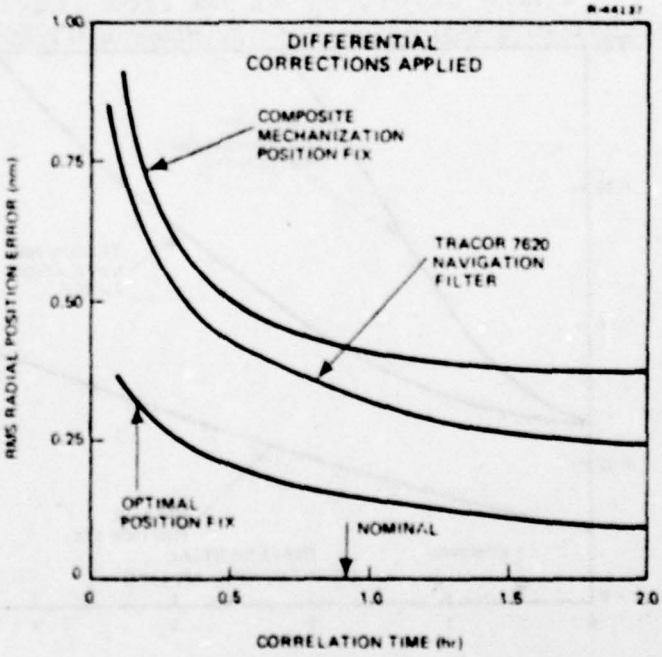

Figure 13 Sensitivity of RMS Radial Position Error to Correlation Time, τ_1 (2 nm from Inuvik)

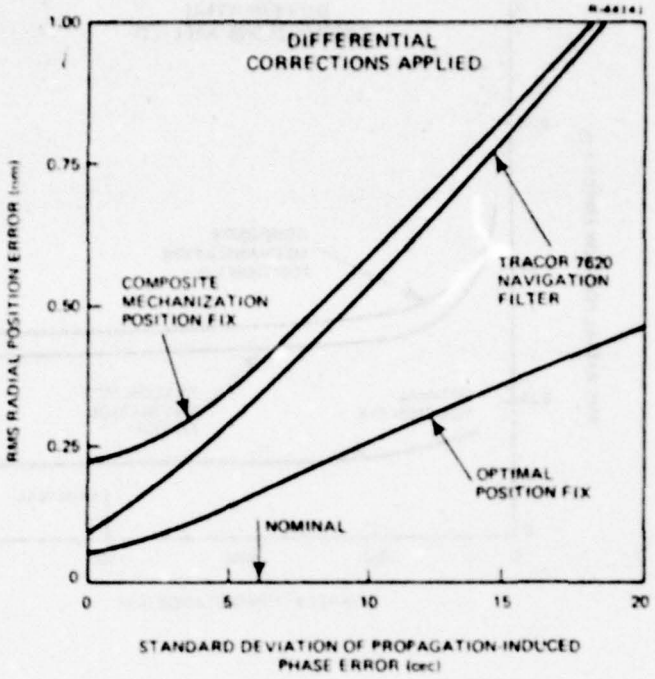

Figure 14 Sensitivity of RMS Radial Position Error to Standard Deviation of Propagation-Induced Phase Error, σ_ϕ (2 nm from Inuvik)

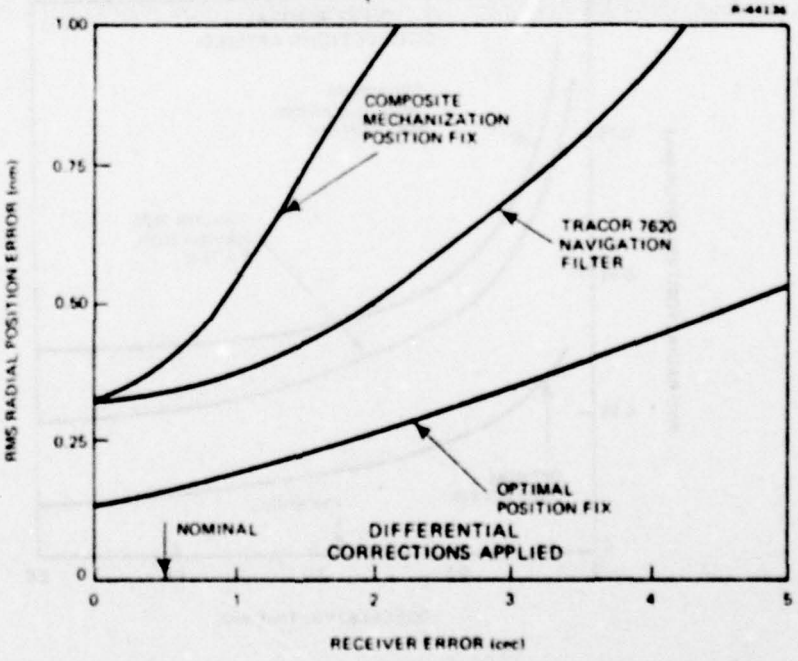

Figure 15 Sensitivity of RMS Radial Position Error to Receiver Error (2 nm from Inuvik)

3.3 USE AS AN ENROUTE AID

In the previous section, performance of the differential Omega system on an approach to Inuvik was evaluated. In this section, the performance of differential Omega is evaluated for a flight away from Inuvik (and consequently, away from a monitor site). Section 3.3.1 describes navigation performance while the aircraft is within range of the monitor update signal. Section 3.3.2 evaluates the alternatives when a differential update is no longer receivable. Section 3.3.3 provides a summary of recommended enroute uses of differential Omega.

3.3.1 Enroute Performance Within Monitor Range

It is assumed that a differential correction can be received up to 125 nm from the monitor. Figure 16 shows navigation performance as a function of distance from the monitor, up to 125 nm. Performance degrades because of spatial decorrelation of the monitor information, but the differential correction still significantly improves performance.

3.3.2 Enroute Performance Beyond Monitor Range

When a differential update can no longer be received, three operational options are considered:

Option 1: Apply the last differential update received as if it were current.

Option 2: Use the last differential correction to calibrate the onboard Predicted Propagation Corrections (PPCs) at the monitor site and use the calibration to adjust PPCs at the indicated aircraft position.

Option 3: Ignore the monitor information and navigate using PPCs.

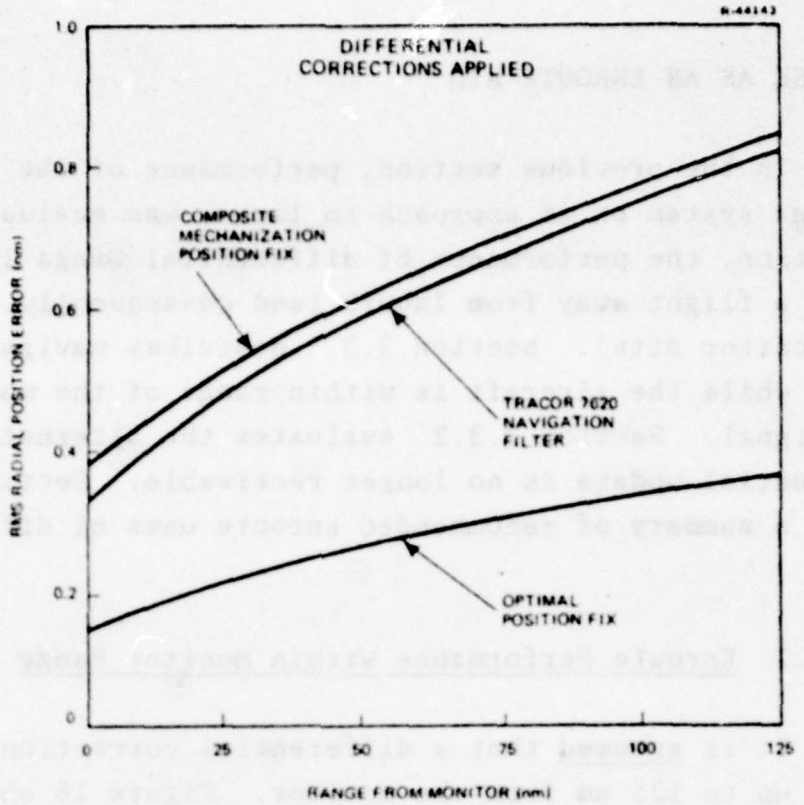

Figure 16 Navigation Performance Within Range of Monitor Updates

Performance under these three options is evaluated below:

Option 1 - There are attractive reasons for continuing to apply the last received differential correction. Such a policy is easy to implement, since it does not require PPC calculations. PPCs are known to be highly correlated in space, suggesting that the differential correction also contains useful information for some distance from the monitor receiver. However, PPCs exhibit rather significant temporal variations. To test the effect of temporal PPC variations on position error, a simulation was run with the following conditions:

- Initial position: 64.5°N, 147.5°W
- Airspeed: 250 kt

- Track: 0°
- Signals from transmitting stations A, C, D, and H assumed to be available
- Noise-free reception assumed
- Include phase shifts corresponding to 2100-2200 GMT, 23 December
- Assume that the last differential correction is obtained at the initial time and position
- Assume that the filter does not apply PPCs.

The simulated conditions characterize very large, probably worst case, PPC changes. There are other dates and times when the simulated effect is minor. However, it is clear from Fig. 17 that this option for area navigation can give rise to unacceptably large errors, regardless of other effects present.

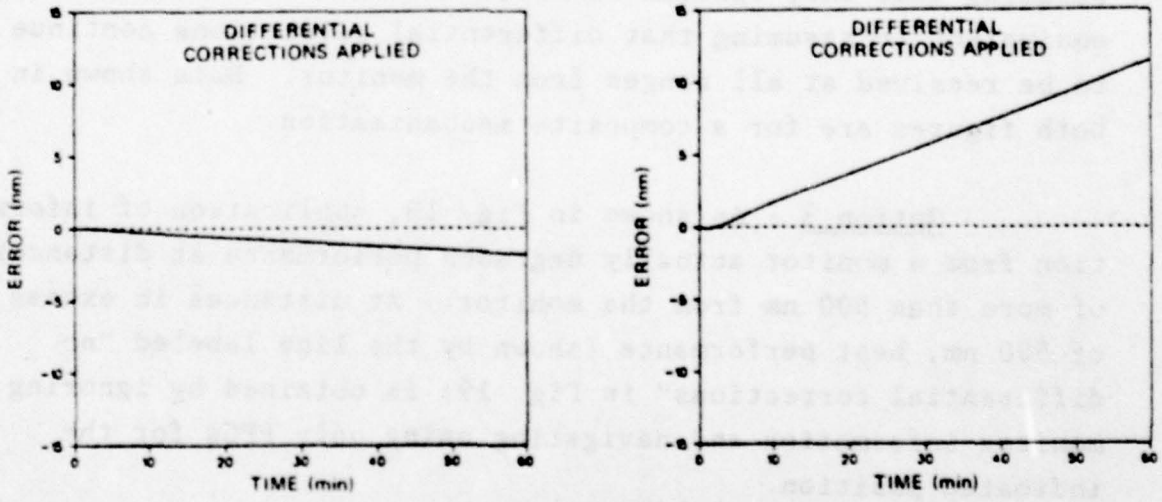

a) North Position Error

b) East Position Error

Figure 17 Effect of Uncompensated PPC

Option 2 - This option requires the Omega navigation set to compute two PPCs for each differential Omega measurement: one for the estimated current position of the aircraft, and one for the location of the monitor. By removing the monitor PPC from the differential update and replacing it with the aircraft PPC, performance degradation caused by changes in the PPCs between the monitor and the aircraft is avoided. Figure 18 (solid curves) shows that this technique provides improved performance for up to 1.5 hr after the last differential update compared to performance with no differential update. This improvement is possible because of the relatively long temporal correlation of residual propagation error information in the monitor update. Assuming an aircraft speed of 250 kt, Fig. 19 (solid curves) shows that monitor information provides improved performance up to 500 nm from the monitor. The dashed curve in Fig. 18 shows performance in the hypothetical case that temporal decorrelation alone is present, which is equivalent to assuming that the aircraft remains 125 nm from the monitor. In Fig. 19 the dashed curve shows performance assuming that only spatial decorrelation occurs, which is equivalent to assuming that differential corrections continue to be received at all ranges from the monitor. Data shown in both figures are for a composite mechanization.

Option 3 - As shown in Fig. 19, application of information from a monitor actually degrades performance at distances of more than 500 nm from the monitor. At distances in excess of 500 nm, best performance (shown by the line labeled "no differential corrections" in Fig. 19) is obtained by ignoring monitor information and navigating using only PPCs for the indicated position.

3.3.3 Summary

Table 7 summarizes the recommended techniques for enroute navigation. A relatively high degree of confidence can be placed in the recommended techniques for short range,

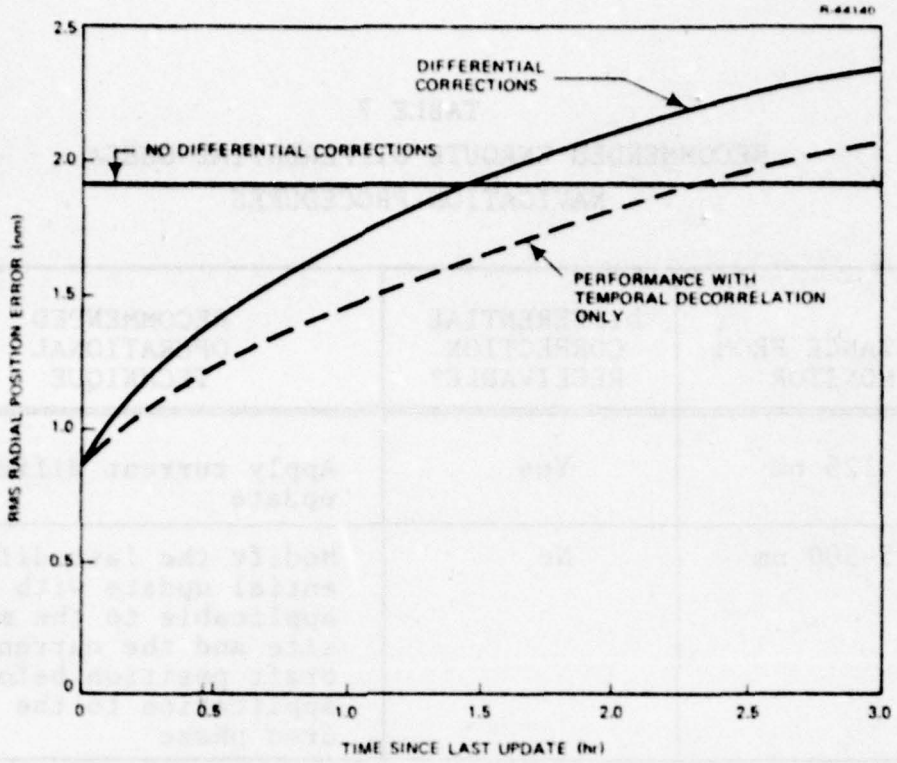

Figure 18 Navigation Performance as a Function of "Staleness" of Monitor Update

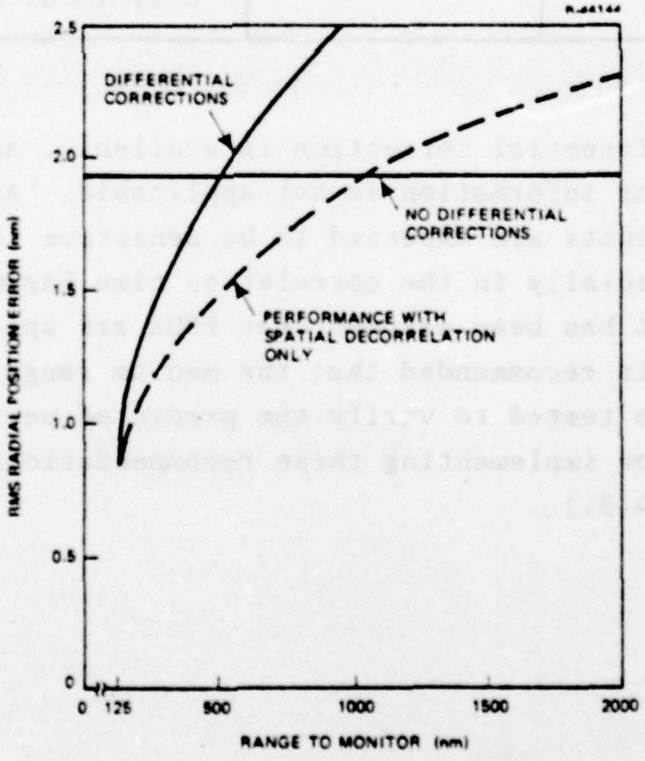

Figure 19 Navigation Performance as a Function of Range to the Monitor

TABLE 7

RECOMMENDED ENROUTE DIFFERENTIAL OMEGA NAVIGATION PROCEDURES

T3441

DISTANCE FROM MONITOR	DIFFERENTIAL CORRECTION RECEIVABLE?	RECOMMENDED OPERATIONAL TECHNIQUE
< 125 nm	Yes	Apply current differential update
125-500 nm	No	Modify the last differential update with PPCs applicable to the monitor site and the current aircraft position before application to the measured phase
>500 nm	No	Ignore the monitor information and navigate using only local PPCs

where a differential correction is available, and long range, where monitor information is not applicable. At medium range, however, results are expected to be sensitive to modeling errors, especially in the correlation time parameter τ_1. In addition, it has been assumed that PPCs are applied with no error. It is recommended that the medium range navigation technique be tested to verify the predicted performance. (An algorithm for implementing these recommendations is described in Section 4.3.)

4. IMPLEMENTATION IN ALASKA

Principal requirements for implementing a differential Omega navigation system in Alaska which is capable of supporting the non-precision approach criteria are described in this chapter. Recommendations are based on a comparison of results presented in Chapter 3 with specific navigation accuracy requirements described in Section 4.1.

4.1 ACCURACY REQUIREMENTS

4.1.1 Overview

Navigation accuracy requirements have been established by the FAA for aircraft using the National Airspace System (NAS). The accuracy requirements fulfill two purposes: to ensure safe operation of individual aircraft and to provide control of the airspace to afford maximum-density, safe operation for multiple users.

Two distinct categories of system navigation accuracy requirements can be identified:

- Certification requirements
- Airspace planning requirements.

Each category has its own particular application.

Certification requirements are established by the FAA in order to qualify equipment for particular applications.

Certification requirements relate to equipment and represent the most stringent category of accuracy requirements. An example of certification requirements are those contained in Ref. 8 for use in certifying Area Navigation Systems.

Airspace planning requirements are used by the FAA in establishing procedures for aircraft to follow in particular circumstances; e.g., in preparing a Standard Instrument Departure (SID) or a Standard Terminal Arrival Route (STAR). These requirements represent planning factors associated with particular equipment configurations and are used to route traffic around obstacles, define Minimum Descent Altitudes (MDA), and establish navigation fixes (e.g., Initial Approach Fix (IAF) and Final Approach Fix (FAF)). Planning requirements are used in documents like Ref. 6 to aid in designing airspace control procedures.

Both types of navigation accuracy requirements are pertinent to the discussion of the Alaska/Yukon differential Omega experiment. If a differential Omega system does not meet certification requirements under the Area Navigation category, the system cannot be used as a primary means of navigation. Regardless of what accuracy can be achieved, it must be quantified in terms of planning requirements before procedures can be developed for use of differential Omega in the NAS.

4.1.2 Non-Precision Approach Aid

By definition, use of a differential Omega navigation system as an approach aid falls in the non-precision approach category; no provision has been made to generate an electronic glide slope. Instrument certification requirements for non-precision approach from Ref. 8 are 0.30 nm along-track and 0.34

nm cross-track* with 95% probability. For definiteness in this report, these accuracy requirements are applied for an FAF at 2 nm from the airport facility.

Procedural requirements are defined by system capabilities. Therefore, the data presented in Chapter 3 of this report specify the procedural accuracy requirements for a differential Omega system. For comparison, the IAF for VOR approach to Deadhorse, Alaska corresponds to 0.63 nm (95%) along-track and 0.50 nm (95%) cross-track according to the criteria of the Ref. 6.

4.1.3 Enroute Aid

The instrument certification requirements for enroute navigation from Ref. 8 are 1.5 nm (95%) for both along-track and cross-track components. Procedural requirements are not applicable in this category.

4.1.4 Summary

Two types of navigation accuracy requirements apply to the differential Omega experiment: certification under Area Navigation requirements (Ref. 8) and procedural requirements as used in the planning documents (Ref. 6). These requirements are summarized in Table 8. The procedural requirements data is an example obtained by analyzing the IAF for a VOR approach to Deadhorse, Alaska.

*The allowance for Flight Technical Error (FTE) has been removed from the cross-track error component.

TABLE 8
NAVIGATION ACCURACY REQUIREMENTS (95% PROBABILITY)

AID CATEGORY	COMPONENT	CERTIFICATION	PROCEDURAL EXAMPLE
Non-Precision Approach	Along-Track Error, nm	0.30	0.63
	Cross-Track Error, nm	0.34	0.50
Enroute	Along-track Error, nm	1.50	NA†
	Cross-track Error, nm	1.50	NA†

†NA = Not Applicable.

4.2 THE ALASKA EXPERIMENTAL EQUIPMENT

Three types of equipment are needed to support the use of differential Omega as a non-precision approach aid:

- Ground station equipment
- Data link equipment
- Airborne navigation equipment.

Descriptions of each of these equipment categories are presented below.

4.2.1 Ground Station Equipment

Ground station equipment must include Omega monitor receivers, data processing and formatting equipment. The ground

station configuration designed for the Alaska/Yukon experiment is considered adequate to support certification of differential Omega as a non-precision approach aid if it is increased to provide a full eight-station capability*. Nevertheless, the analysis presented in previous chapters validates the requirement for certain design features of this equipment which deserve special emphasis:

- Precision local oscillator at the monitor (Rubidium standard)
- Nearly continuous phase and amplitude data (every 10 sec)
- Some filtering of data prior to transmission (average data for five min).

(Actual equipment characteristics are shown in parentheses.)

The monitor receivers used in the differential Omega experiment are standard TRACOR 599R receivers which have been modified to provide a digital phase output. The receivers are augmented by a precision, external atomic frequency standard. Therefore, the receivers are capable of measuring single station Omega phase, and independent differential phase corrections can be generated for each Omega signal.

The monitors also provide nearly continuous phase and amplitude data. The data are filtered to smooth out noise and then sent to the data formatting equipment. The effect of this filtering is depicted in Fig. 10.

Signal amplitude data are used in the ground station equipment to derive a signal-quality index. This index allows the airborne equipment to determine the quality of differential corrections and avoid processing signals which are unreliable.

---

*The experiment will use only signals from Norway, Hawaii, North Dakota and Japan.

Differential corrections are computed by subtracting the received Omega phase from the nominal phase for the monitor site. The correction is then formatted and inserted in the data message. New corrections are computed every 10 sec.

4.2.2 Data Link

The data link designed for the differential Omega experiment in Alaska appears to be adequate to support certification requirements for a non-precision approach aid. The message format should be expanded to allow correction processing for all eight Omega transmitting stations, but sufficient channel capacity exists for this modification. (The design channel capacity provides an information rate of 60 characters per sec.)

4.2.3 Airborne Navigation Equipment

Performance predictions contained in Chapter 3 indicate that the TRACOR 7620 receiver may meet certification requirements as an enroute aid to navigation under the criteria of Ref. 8. Uncertainty in the value of the correlation coefficient, ρ, which cannot be resolved without processing data from the experiment, provides a range of accuracy numbers; e.g., cross-track position error near Inuvik is 1.2 nm (95%)* for ρ=0.9 and 2.3 nm (95%) for ρ=0.5 compared to a requirement of 1.5 nm. The true correlation coefficient is thought (see Appendix B) to be much nearer 1.0 than 0.5, and ρ=0.9 may provide reasonable predictions of the TRACOR 7620 navigation set performance.

---

*The results in Chapter 3 are expressed as rms errors. For a joint Gaussian distribution with zero-mean, identically distributed, independent components, 95% probability corresponds to a circle of radius 2.45 times the standard deviation, σ, of each component. The 95% region for a single Gaussian distribution is $\pm 1.96\sigma$.

The predictions in Chapter 3 indicate that the accuracy obtainable with the TRACOR 7620 receiver in the differential Omega configuration does not meet certification requirements as a non-precision approach aid under the criteria of Ref. 8. For example, the cross-track error ranges between 0.31 and 0.49 nm (95%) as compared to a requirement of 0.30 nm. (95%). Nevertheless, two alternate implementations are available which offer the potential to meet certification requirements: operation with 13.6 kHz signals only, and an "optimal" two-frequency implementation. (Both of these mechanizations are discussed in Section 4.3.)

Regardless of how the navigation receiver is mechanized, it must provide additional features to the pilot:

- Waypoint flight path computation
- Guidance display.

The waypoint features of the TRACOR 7620 set are typical of a large number of commercial/military receivers and provide for operator insertion of up to 10 waypoints. The operator can select displays which provide distance-to-go, desired-track-angle, estimated-time-of-arrival, etc. (To be most useful, FAA-developed SID and STAR procedures would include tabulated coordinates for procedural waypoints.) These displays offer guidance information to the pilot, but more standard control features are desirable; e.g., outputs to drive a course deviation indicator or radio magnetic indicator.

4.3 OTHER EXISTING EQUIPMENT

The equipment constructed for the differential Omega experiment in the Alaska/Yukon region is believed to be the

only equipment currently available for use in an airborne application. All of the equipment is special-purpose, and of a developmental nature.

During the course of this contract, TASC contacted numerous manufacturers of Omega navigation equipment. Many of them expressed an interest in the potential market, but none disclosed plans to develop or market receiver equipment in the near future. The primary concerns expressed by equipment manufacturers were an uncertainty in the size of the potential market, the absence of plans and standards for ground station and data link equipments, and the marginal nature of Omega coverage in large sections of the continental United States.

At the same time, several manufacturers were eager to discuss their product line of Omega and Omega/VLF communications receivers. These receivers are primarily designed for the commercial market on long over-water flights where VOR/DME signals are unavailable.

4.4 SUGGESTED IMPROVEMENTS

The ground station and data link equipments described in Section 4.1 are adequate to support analytical certification requirements for differential Omega operation in the non-precision approach category if they are modified to provide a full eight-station capability. Nevertheless, experience gained as a result of the experiment may suggest modifications to improve reliability or convenience.

Two alternative approaches to the mechanization of the airborne navigation equipment appear to offer promise:

- Single-frequency operation in the differential Omega mode
- Correction including predicted propagation effects.

Both techniques are described below.

4.4.1 Single-Frequency Operation

The composite Omega procedure used by TRACOR in the 7620 set is designed to reduce receiver sensitivity to certain types of propagation anomalies (e.g., Sudden Ionospheric Disturbances) and to improve performance with a simplified propagation prediction model. Within the differential Omega region, the ground station equipment provides a more accurate means of correcting for these effects, and the performance degradation associated with processing additional independent receiver noise is not offset by a corresponding gain in navigation performance. (The composite mechanization subtracts the phase received on 13.6 kHz from that received at 10.2 kHz. While this reduces propagation errors, it increases the effect of measurement noise because the noise contributions to each frequency are independent.)

For example, compare the position-fix quality in terms of cross-track position errors for the TRACOR composite (ρ=0.9) and the single-frequency (13.6 kHz) mechanizations in Table 4. The rms random propagation errors are nearly equal: 0.16 and 0.14 nm, respectively. The rms receiver errors are substantially different: 0.22 and 0.07 nm, respectively. The total rms errors are 0.27 and 0.16 nm, respectively. This difference is directly attributable to the increased sensitivity of the composite mechanization to receiver noise as compared to the single-frequency mechanization.

The use of single-frequency data in the differential Omega region improves navigation performance for the non-precision approach application, but it does not eliminate the need for a multiple frequency receiver in enroute applications. (Multiple frequencies allow the receiver to resolve much wider lane ambiguities, which might be required after a temporary in-flight electrical power transient.) Multiple frequencies allow better operation outside the differential Omega region and provide potential insensitivity to propagation anomalies.

4.4.2 Propagation Model Correction

If the airborne receiver is supplied the coordinates of the ground station monitor, a propagation model correction algorithm can be implemented which offers the potential for significantly improving the transition from differential Omega to Omega navigation outside the differential Omega region. This is similar to the procedure described in Ref. 9, and it is supported by the results given in Figs. 17 and 18.

The mechanization of a propagation model correction algorithm might have the following form. Denote by $\phi^{c}_{i,j}$ the differential correction broadcast by the ground station for station i on frequency j. Then

$$\phi^{c}_{i,j}(\underline{x},t) = \phi_{i,j}(\underline{x}) - \phi^{m}_{i,j}(\underline{x},t) \qquad (13)$$

where

$\underline{x}$ is the monitor location

t is the measurement instant

$\phi_{i,j}(\underline{x})$ is the nominal Omega phase at $\underline{x}$ for station i at frequency j

$\phi^{m}_{i,j}(\underline{x},t)$ is the measured Omega phase at $\underline{x}$ at instant t

Denote the receiver-computed propagation correction (skywave correction for the TRACOR 7620) by $\phi^{P}_{i,j}(\underline{x},t)$ and define the propagation model correction as follows:

$$\Delta\phi^{P}_{i,j}(t) = \phi^{P}_{i,j}(\underline{x},t) - \phi^{C}_{i,j}(\underline{x},t) \tag{14}$$

If the differential corrections are lost, perhaps because the aircraft has departed the differential Omega region, define a new propagation correction $\phi^{P*}_{i,j}(\underline{y},\lambda)$ (for location $\underline{y}$ and time λ larger than t_o, the time at which new corrections become unavailable) according to

$$\phi^{P*}_{i,j}(\underline{y},\lambda) = \phi^{P}_{i,j}(\underline{y},\lambda) - \beta\Delta\phi^{P}_{i,j}(t_o) \tag{15}$$

where β is a weighting factor.

A candidate algorithm for computing β, which is consistent with the data in Chapter 3, is

$$\beta = e^{-(\lambda - t_o)/T_m} \tag{16}$$

where T_m is a memory constant. The choice of T_m depends on a number of factors including the Omega characteristics of the operating region and the flight characteristics of the aircraft. (A reasonable value for T_m is expected to be 45 min.)

The algorithm described by Eqs. 14 through 16 provides <u>one</u> method for implementing the recommendations of Section 3.3. It has the advantage that the transition between applying a phase monitor correction and operating only with computed propagation corrections is smooth, and the pilot will not experience rapid jumps in the indicated Omega position. The potential

disadvantages of the algorithm are that it has not been tested and it may be sensitive to assumptions about the nominal parameter values in the Omega phase error model.

5. CONCLUSIONS

This report presents the results of an analytic evaluation of the differential Omega experiment in the Alaska/Yukon region. Primary emphasis is placed on the particular equipment, installation and procedures peculiar to this experiment. The analysis also includes an assessment of the expected performance of an "optimal" two-frequency receiver using the experimental differential Omega correction format. The latter results provide an analytical justification of the suitability of differential Omega for non-precision approach applications. This analysis is based on a worldwide Omega error model which has not been validated for the Alaska/Yukon region.

Performance results presented in Chapter 3 for nominal parameters of the Omega error model described in Chapter 2, indicate that the experimental differential Omega equipment:

- May not meet certification requirements as an Area Navigation System (Ref. 8) for non-precision approach without further modifications
- Should meet certification requirements as an Area Navigator for enroute navigations
- Will not be adversely affected by the loss of signals from any one of four Omega transmitting stations normally received in the experimental region
- Is expected to maintain adequate Omega signal tracking during standard rate turns.

APPENDIX A
OMEGA PHASE ERROR MODEL

A.1 OPTIMAL OMEGA SIGNAL PROCESSING

A model is developed in this section for the position error resulting from optimal (minimum-variance) usage of phase information from two Omega frequencies, 10.2 kHz and 13.6 kHz, for each of four stations:

- A (Norway)
- C (Hawaii)
- D (North Dakota)
- H (Japan).

Based on the estimated position of the navigation set, an estimated phase $\hat{\phi}_{ij}$ is computed for each station i on each frequency j as follows:

$$\hat{\phi}_{ij} = \frac{\hat{R}_i}{\lambda_j} \qquad \text{(A-1)}$$

where

$\hat{R}_i$ is the range to station i from the estimated position

λ_j is the nominal wavelength of a signal with frequency j

The difference between estimated phase $\hat{\phi}_{ij}$ and measured phase ϕ^m_{ij} is the phase deviation:

$$\Delta\phi_{ij} = \hat{\phi}_{ij} - \phi^{m}_{ij} \qquad \text{(A-2)}$$

Phase deviation is related to position error as follows:

$$\begin{bmatrix} \Delta\phi_{1,10.2} \\ \Delta\phi_{2,10.2} \\ \Delta\phi_{3,10.2} \\ \Delta\phi_{4,10.2} \\ \Delta\phi_{1,13.6} \\ \Delta\phi_{2,13.6} \\ \Delta\phi_{3,13.6} \\ \Delta\phi_{4,13.6} \end{bmatrix} = \begin{bmatrix} \frac{\cos\psi_1}{\lambda_{10.2}} & \frac{\sin\psi_1}{\lambda_{10.2}} \\ \frac{\cos\psi_2}{\lambda_{10.2}} & \frac{\sin\psi_2}{\lambda_{10.2}} \\ \frac{\cos\psi_3}{\lambda_{10.2}} & \frac{\sin\psi_3}{\lambda_{10.2}} \\ \frac{\cos\psi_4}{\lambda_{10.2}} & \frac{\sin\psi_4}{\lambda_{10.2}} \\ \frac{\cos\psi_1}{\lambda_{13.6}} & \frac{\sin\psi_1}{\lambda_{13.6}} \\ \frac{\cos\psi_2}{\lambda_{13.6}} & \frac{\sin\psi_2}{\lambda_{13.6}} \\ \frac{\cos\psi_3}{\lambda_{13.6}} & \frac{\sin\psi_3}{\lambda_{13.6}} \\ \frac{\cos\psi_4}{\lambda_{13.6}} & \frac{\sin\psi_4}{\lambda_{13.6}} \end{bmatrix} \begin{bmatrix} \Delta N \\ \Delta E \end{bmatrix} + \begin{bmatrix} \delta\phi_{1,10.2} \\ \delta\phi_{2,10.2} \\ \delta\phi_{3,10.2} \\ \delta\phi_{4,10.2} \\ \delta\phi_{1,13.6} \\ \delta\phi_{2,13.6} \\ \delta\phi_{3,13.6} \\ \delta\phi_{4,13.6} \end{bmatrix} \qquad \text{(A-3)}$$

where

$\Delta\phi_{ij}$ is the phase deviation from station i on frequency j

ψ_i is the bearing to transmitter i

ΔN is north position error

ΔE is east position error

$\delta\phi_{ij}$ is the phase measurement error from station i on frequency j.

Phase measurement error $\delta\phi_{ij}$ is comprised of phase error from all sources except position error, and includes receiver error, clock synchronization and drift error, and signal propagation prediction error. Note that Eq. A-3 applies in the non-differential mode as well as the differential mode. In the differential mode, a correction from a nearby monitor station is applied to the measured phase ϕ^m_{ij} in an attempt to minimize the phase measurement error $\delta\phi_{ij}$. In the differential mode, $\delta\phi_{ij}$ represents the residual phase measurement error after correction by the monitor.

Equation A-3 can be rewritten as follows:

$$\underline{\Delta\phi} = H\,\underline{\Delta x} + \underline{\delta\phi} \qquad \text{(A-4)}$$

It can be shown (Ref. 10) that the minimum-variance estimate of $\underline{\Delta x}$, given the phase deviations $\underline{\Delta\phi}$ in the presence of phase measurement errors $\underline{\delta\phi}$, is

$$\underline{\Delta\hat{x}} = (H^T R^{-1} H)^{-1} H^T R^{-1} \underline{\Delta\phi} \qquad \text{(A-5)}$$

where $R \triangleq E[\underline{\delta\phi}\ \underline{\delta\phi}^T]$ and $E[\cdot]$ is the expectation operator. The covariance of the estimate $\underline{\Delta\hat{x}}$ is computed as follows:

$$P = (H^T R^{-1} H)^{-1} \qquad \text{(A-6)}$$

where

$$P \triangleq E[(\underline{\Delta\hat{x}} - \underline{\Delta x})(\underline{\Delta\hat{x}} - \underline{\Delta x})^T]$$

To evaluate the variance in the estimate of position error an expression for the matrix R is required.

To determine R, consider $\delta\phi_{ij}$, the phase measurement error from station i on frequency j caused by all sources except position error. Assume that the navigator is at position $\underline{x}_1$ and obtains a phase measurement at time t_1. Then the measured phase can be expressed by

$$\phi^m_{ij}(\underline{x}_1, t_1) = \phi_{ij}(\underline{x}_1) + \delta\phi_{ij}(\underline{x}_1, t_1) \qquad \text{(A-7)}$$

or

$$\phi^m_{ij}(\underline{x}_1, t_1) = \phi_{ij}(\underline{x}_1) + \delta\phi^p_{ij}(\underline{x}_1, t_1) + \delta\phi^r_{ij}(\underline{x}_1, t_1) + \delta\phi^c_{ij}(\underline{x}_1, t_1) + \delta\phi^v_{ij}(\underline{x}_1, t_1) \qquad \text{(A-8)}$$

where

- ϕ^m_{ij} is the measured phase from station i on frequency j
- ϕ_{ij} is the "nominal" phase determined from range to transmitter and signal wavelength
- $\delta\phi_{ij}$ is phase measurement error caused by all sources except position error
- $\delta\phi^p_{ij}$ is the phase perturbation caused by predictable propagation effects
- $\delta\phi^r_{ij}$ is the phase error caused by unpredictable (random) propagation error
- $\delta\phi^c_{ij}$ is the constant offset portion of measured phase introduced by the receiver (i.e., clock error)
- $\delta\phi^v_{ij}$ is the variable offset portion of the measured phase introduced by the receiver (receiver noise)

Assume that a monitor measures phase at position $\underline{x}_2$ at time t_2. The measured phase at the monitor is given by

$$\phi^{m}_{ij}(\underline{x}_2,t_2) = \phi_{ij}(\underline{x}_2) + \delta\phi^{p}_{ij}(\underline{x}_2,t_2) + \delta\phi^{r}_{ij}(\underline{x}_2,t_2)$$

$$+ \delta\phi^{c}_{ij}(\underline{x}_2,t_2) + \delta\phi^{v}_{ij}(\underline{x}_2,t_2) \qquad \text{(A-9)}$$

The monitor correction, transmitted to the navigator, is measured phase minus nominal phase:

$$\text{CORRECTION} = \phi^{m}_{ij}(\underline{x}_2,t_2) - \phi_{ij}(\underline{x}_2)$$

$$= \delta\phi^{p}_{ij}(\underline{x}_2,t_2) + \delta\phi^{r}_{ij}(\underline{x}_2,t_2) + \delta\phi^{c}_{ij}(\underline{x}_2,t_2)$$

$$+ \delta\phi^{v}_{ij}(\underline{x}_2,t_2) \qquad \text{(A-10)}$$

The navigation set receives the correction and uses it to estimate nominal phase as follows:

$$\hat{\phi}_{ij}(\underline{x}_1,t_1) = \phi^{m}_{ij}(\underline{x}_1,t_1) - \text{CORRECTION} \qquad \text{(A-11)}$$

Substituting Eq. A-10 into Eq. A-11 yields

$$\hat{\phi}_{ij}(\underline{x}_1,t_1) = \phi^{m}_{ij}(\underline{x}_1,t_1) - \delta\phi^{p}_{ij}(\underline{x}_2,t_2) - \delta\phi^{r}_{ij}(\underline{x}_2,t_2)$$

$$- \delta\phi^{c}_{ij}(\underline{x}_2,t_2) - \delta\phi^{v}_{ij}(\underline{x}_2,t_2) \qquad \text{(A-12)}$$

Combining Eqs. A-12 and A-8 yields an expression for the error in measured phase at the receiver:

$$\delta\phi_{ij}(\underline{x}_1,t_1) = \hat{\phi}_{ij}(\underline{x}_1,t_1) - \phi_{ij}(\underline{x}_1)$$

$$= \delta\phi^{p}_{ij}(\underline{x}_1,t_1) - \delta\phi^{p}_{ij}(\underline{x}_2,t_2)$$

$$+ \delta\phi^{r}_{ij}(\underline{x}_1,t_1) - \delta\phi^{r}_{ij}(\underline{x}_2,t_2)$$

$$+ \delta\phi^{c}_{ij}(\underline{x}_1,t_1) - \delta\phi^{c}_{ij}(\underline{x}_2,t_2)$$

$$+ \delta\phi^{v}_{ij}(\underline{x}_1,t_1) - \delta\phi^{v}_{ij}(\underline{x}_2,t_2) \qquad \text{(A-13)}$$

Equation A-13 shows that measured phase error depends only on the difference in the four types of errors at the navigator and the monitor. The monitor is effective because the terms $\delta\phi^{p}_{ij}$ and $\delta\phi^{r}_{ij}$ change relatively little over short distances and short time intervals; i.e., these errors are highly correlated in time and space. The other terms, $\delta\phi^{c}_{ij}$ and $\delta\phi^{v}_{ij}$, which are uncorrelated between the monitor and the navigator, must be relatively small for the monitor to be effective. Equation A-13 is used to compute the matrix R.

The following assumptions simplify the analysis:

1. $\delta\phi^{p}_{ij}(\underline{x}_2,t_2) = \delta\phi^{p}_{ij}(\underline{x}_1,t_1)$. PPCs are assumed to not change over the distance $|\underline{x}_2-\underline{x}_1|$ and the time $|t_2-t_1|$.

2. $\delta\phi^{c}_{ij}(\underline{x}_2,t_2) - \delta\phi^{c}_{ij}(\underline{x}_1,t_1) = 0$. Any bias offset in phase introduced by the receiver is assumed to be negligible.

3. $E[\delta\phi^{r}_{ij}\ \delta\phi^{v}_{ij}] = 0$. Random propagation anomalies are assumed to be uncorrelated with receiver noise.

4. $E[\delta\phi_{ij}\ \delta\phi_{kj}] = 0$. Any two errors involving two different transmitters are assumed to be uncorrelated.

Under these assumptions, it can be shown that the matrix R is comprised of common-frequency terms, of the form $E\{[\delta\phi_{ij}]^2\}$, and cross-frequency terms, of the form $E[\delta\phi_{ij}\ \delta\phi_{ik}]$.

Common-frequency terms are in turn composed of two types of terms: receiver error and random propagation error. The model for variable receiver error is chosen to be a discrete white noise sequence with a variance of

$$E\{[\delta\phi^{v}_{ij}(\underline{x},t)]^2\} = \sigma_v^2 \qquad \text{(A-14)}$$

The assumed model for random propagation error is adapted from Ref. 6 and applies to the case $t_2 - t_1 < 2$ hr for a frequency of 10.2 kHz:

$$E\{[\delta\phi^{r}_{i,10.2}(\underline{x}_2,t_2)]\,[\delta\phi^{r}_{i,10.2}(\underline{x}_1,t_1)]\}$$

$$= \exp\left(-\frac{|\underline{x}_2 - \underline{x}_1|}{d}\right)\left\{\sigma_1^2 \exp\left(\frac{|t_2 - t_1|}{\tau_1}\right) + \sigma_2^2\right.$$

$$\left. + \sigma_3^2 \cos\left(\frac{2\pi}{T_3}|t_2 - t_1|\right) + \sigma_4^2 \cos\left(\frac{2\pi}{T_4}|t_2 - t_1|\right)\right\} \qquad \text{(A-15)}$$

where

$d = 1500$ nm $\qquad \sigma_1^2 = 9.83$ cec^2

$\tau_1 = 0.943$ hr $\qquad \sigma_2^2 = 17.8$ cec^2

$T_3 = 12$ hr $\qquad \sigma_3^2 = 8.13$ cec^2

$T_4 = 8$ hr $\qquad \sigma_4^2 = 1.98$ cec^2

The model is calibrated with data at 10.2 kHz. At 13.6 kHz, it is assumed that the same functional form applies but includes a weighting factor, W:

$$E\{[\delta\phi^r_{i,13.6}(\underline{x}_2,t_2)]\ [\delta\phi^r_{i,13.6}(\underline{x}_1,t_1)]\}$$

$$= W^2 \exp\left(-\frac{|\underline{x}_2 - \underline{x}_1|}{d}\right)\left\{\sigma_1^2 \exp\left(\frac{|t_2 - t_1|}{\tau_1}\right)\right. \qquad \text{(A-16)}$$

$$\left. + \sigma_2^2 + \sigma_3^2 \cos\left(\frac{2\pi}{T_3}|t_2 - t_1|\right) + \sigma_4^2 \cos\left(\frac{2\pi}{T_4}|t_2 - t_1|\right)\right\}$$

Cross-frequency terms involve only random propagation error. From Eqs. A-15 and A-16, it can be shown that the cross-frequency term is given by:

$$E\{[\delta\phi^r_{ij}(\underline{x}_2,t_2)]\ [\delta\phi^r_{ik}(\underline{x}_1,t_1)]\}$$

$$= \rho W \exp\left(-\frac{|\underline{x}_2 - \underline{x}_1|}{d}\right)\left\{\sigma_1^2 \exp\left(\frac{|t_2 - t_1|}{\tau_1}\right)\right.$$

$$+ \sigma_2^2 + \sigma_3^2 \cos\left(\frac{2\pi}{T_3}|t_2 - t_1|\right)$$

$$\left. + \sigma_4^2 \cos\left(\frac{2\pi}{T_4}|t_2 - t_1|\right)\right\}$$

$$\text{for } j \neq k \qquad \text{(A-17)}$$

where ρ is the correlation coefficient between frequencies.

The matrix R is composed of common- and cross-frequency terms as follows:

$$R = \begin{bmatrix} R_1 & 0 & 0 & 0 & R_3 & 0 & 0 & 0 \\ 0 & R_1 & 0 & 0 & 0 & R_3 & 0 & 0 \\ 0 & 0 & R_1 & 0 & 0 & 0 & R_3 & 0 \\ 0 & 0 & 0 & R_1 & 0 & 0 & 0 & R_3 \\ R_3 & 0 & 0 & 0 & R_2 & 0 & 0 & 0 \\ 0 & R_3 & 0 & 0 & 0 & R_2 & 0 & 0 \\ 0 & 0 & R_3 & 0 & 0 & 0 & R_2 & 0 \\ 0 & 0 & 0 & R_3 & 0 & 0 & 0 & R_2 \end{bmatrix}$$

where

$$R_1 = E\{[\delta\phi^v_{ij}(\underline{x}_2,t_2)]^2\} + E\{[\delta\phi^v_{ij}(\underline{x}_1,t_1)]^2\}$$

$$+ 2E\{[\delta\phi^r_{i,10.2}(\underline{x},t)]^2\}$$

$$- 2E\{[\delta\phi^r_{i,10.2}(\underline{x}_2,t_2)]\ [\delta\phi^r_{i,10.2}(\underline{x}_1,t_1)]\}$$

$$R_2 = E\{[\delta\phi^v_{ij}(\underline{x}_2,t_2)]^2\} + E\{[\delta\phi^v_{ij}(\underline{x}_1,t_1)]^2\}$$

$$+ 2E\{[\delta\phi^r_{i,13.6}(\underline{x},t)]^2\}$$

$$- 2E\{[\delta\phi^r_{i,13.6}(\underline{x}_2,t_2)]\ [\delta\phi^r_{i,13.6}(\underline{x}_1,t_1)]\}$$

$$R_3 = 2E\{[\delta\phi^r_{ij}(\underline{x},t)]\ [\delta\phi^r_{ik}(\underline{x},t)]\}$$

$$- 2E\{[\delta\phi^r_{ij}(\underline{x}_2,t_2)]\ [\delta\phi^r_{ik}(\underline{x}_1,t_1)]\} \qquad (j\neq k)$$

A.2 TRACOR COMPOSITE SIGNAL PROCESSING

In the previous section, the covariance of the position estimation error was derived (Eq. A-6) assuming optimal use of eight phase measurements (Eq. A-3). In this section, the covariance of the position estimation error is calculated assuming the eight phase measurements to be combined as in the TRACOR 7620 receiver to form three "composite" phases of the form

$$\phi_{ij,c} = a(\phi_{i,13.6} - \phi_{j,13.6}) - b(\phi_{i,10.2} - \phi_{j,10.2}) \qquad \text{(A-18)}$$

where

$\Phi_{ij,c}$ is the composite phase from transmitters i and j

$\Phi_{i,13.6}$ is the phase from transmitter i on frequency 13.6 kHz

$\Phi_{j,10.2}$ is the phase from transmitter j on frequency 10.2 kHz

a,b are constants (a = 15/8, b = 3/2)

In analogy to Section A.1, composite phase deviation, $\Delta\Phi_{ij,c}$, is related to position error as follows

$$\begin{bmatrix} \Delta\Phi_{12,c} \\ \Delta\Phi_{13,c} \\ \Delta\Phi_{14,c} \end{bmatrix} = \frac{1}{\lambda_c} \begin{bmatrix} \cos\psi_1 - \cos\psi_2 & \sin\psi_1 - \sin\psi_2 \\ \cos\psi_1 - \cos\psi_3 & \sin\psi_1 - \sin\psi_3 \\ \cos\psi_1 - \cos\psi_4 & \sin\psi_1 - \sin\psi_4 \end{bmatrix} \begin{bmatrix} \Delta N \\ \Delta E \end{bmatrix} + \begin{bmatrix} \delta\Phi_{12,c} \\ \delta\Phi_{13,c} \\ \delta\Phi_{14,c} \end{bmatrix} \quad \text{(A-19)}$$

where

$$\delta\Phi_{ij,c} = a(\delta\Phi_{i,13.6} - \delta\Phi_{j,13.6}) - b(\delta\Phi_{i,10.2} - \delta\Phi_{j,10.2})$$

$$\lambda_c = \left(\frac{a}{\lambda_{13.6}} - \frac{b}{\lambda_{10.2}}\right)^{-1} = \text{composite wavelength}$$

Phase measurement error $\delta\Phi_{ij}$ (j = 13.6 or 10.2) is given in Section A.1 (Eq. A-13).

Equation A-19 can be written in the form

$$\underline{\Delta\Phi}_c = H_c \, \underline{\Delta x} + \underline{\delta\Phi}_c \quad \text{(A-20)}$$

The minimum variance estimate of $\underline{\Delta x}$ is then given by

$$\underline{\Delta \hat{x}} = (H_c^T R_c^{-1} H_c)^{-1} H_c^T R_c^{-1} \underline{\Delta \phi}_c \qquad \text{(A-21)}$$

where

$$R_c = E[\underline{\delta\phi}_c \ \underline{\delta\phi}_c^T]$$

The covariance of $\underline{\Delta \hat{x}}$, which represents a lower bound for the covariance of position error resulting from a single set of three composite phase measurements using the TRACOR 7620 algorithm, is given by:

$$P_c = (H_c^T R_c^{-1} H_c)^{-1} \qquad \text{(A-22)}$$

The matrix R_c can be determined in a manner similar to the method in Section A.1 and has two types of terms:

- Diagonal, $E\{[\delta\phi_{ij,c}]^2\}$
- Off-diagonal, $E\{[\delta\phi_{ij,c}]\ [\delta\phi_{ik,c}]\}$, $j \neq k$

Diagonal terms are given by:

$$\begin{aligned} E\{[\delta\phi_{ij,c}]^2\} = {} & 4b^2\, E\{[\delta\phi^r_{i,10.2}(\underline{x},t)]^2\} \\ & - 4b^2\, E\{[\delta\phi^r_{i,10.2}(\underline{x}_2,t_2)]\ [\delta\phi^r_{i,10.2}(\underline{x}_1,t_1)]\} \\ & + 4a^2\, E\{[\delta\phi^r_{i,13.6}(\underline{x}_1,t)]^2\} \\ & - 4a^2\, E\{[\delta\phi^r_{i,13.6}(\underline{x}_2,t_2)]\ [\delta\phi^r_{i,13.6}(\underline{x}_1,t_1)]\} \\ & - 8ab\, E\{[\delta\phi^r_{i,13.6}(\underline{x},t)]\ [\delta\phi^r_{i,10.2}(\underline{x},t)]\} \end{aligned}$$

$$+ 8ab\ E\{[\delta\phi^r_{ij}(\underline{x}_2,t_2)]\ [\delta\phi^r_{ik}(\underline{x}_1,t_1)]\}$$

$$+ 2(a^2 + b^2)\ E\{[\delta\phi^v_{ij}(\underline{x}_2,t_2)]^2\}$$

$$+ 2(a^2 + b^2)\ E\{[\delta\phi^v_{ij}(\underline{x}_1,t_1)]^2\}$$

$$\text{for } (j \neq k) \qquad \text{(A-23)}$$

Terms on the right side of Eq. A-23 are given by Eqs. A-14, A-15, A-16, A-17. Off-diagonal terms are equal to one-half the diagonal terms:

$$E\{[\delta\phi_{ij,c}]\ [\delta\phi_{ik,c}]\} = \tfrac{1}{2}\ E\{[\delta\phi_{ij,c}]^2\},\ j \neq k \qquad \text{(A-24)}$$

The matrix R_c is written as follows:

$$R_c = \begin{bmatrix} R_{c1} & R_{c2} & R_{c2} \\ R_{c2} & R_{c1} & R_{c2} \\ R_{c2} & R_{c2} & R_{c1} \end{bmatrix} \qquad \text{(A-25)}$$

where

$$R_{c1} = E\{[\delta\phi_{ij,c}]^2\}$$

$$R_{c2} = E\{[\delta\phi_{ij,c}]\ [\delta\phi_{ik,c}]\},\ j \neq k$$

APPENDIX B

FREQUENCY CORRELATION OF OMEGA ERRORS

This appendix presents the approach used to provide a statistical prediction of the cross-frequency correlation between the propagation medium-induced random phases of 10.2 and 13.6 kHz Omega signals. Both the 10.2 and 13.6 kHz signals are assumed to be radiated by the same Omega transmitter and received simultaneously* at the same measurement site. The equation for the cross-frequency correlation coefficient is

$$\rho_{10.2,13.6} = \frac{E[\delta\phi_{10.2}\ \delta\phi_{13.6}]}{E[(\delta\phi_{10.2})^2]\ E[(\delta\phi_{13.6})^2]} \qquad \text{(B-1)}$$

where

$\delta\phi_{10.2}$ is the propagation-medium-induced random phase in the 10.2 kHz signals

$\delta\phi_{13.6}$ is the propgation-medium-induced random phase in the 13.6 kHz signals.

At a given receiver location, the phase of a received Omega (or VLF) signal is a function of signal frequency, signal (i.e., transmitter-to-receiver) path length, and propagation medium properties along this path such as ground conductivity, geomagnetic latitude, bearing angle and the (D-region) ionosphere. The ionosphere properties vary significantly with the solar zenith angle along the path. The primary source of propagation-medium-induced random signal phase is the random temporal

*The one-second delay between successive Omega bursts is negligible in this context.

variations in the properties of the ionosphere along the path. Therefore, the subsequent random phase analysis considers only random changes in the ionosphere properties.

At VLF, the D-region ionosphere properties are adequately characterized, according to Wait and Spies (Ref. 11), by two parameters: the ionosphere reflection layer height, h, and the ionospheric conductivity gradient, β. According to Kelly (Ref. 12), each parameter can be assumed to be independently variable and characterized by a Gaussian probability distribution. The frequently-used values for the mean and standard deviation of the ionospheric parameters are given in Table B-1 (Refs. 12 and 13), for both day paths (i.e., local-noon conditions along the entire path) and night paths (complete darkness along the entire path). The mean values correspond to a "quiet" ionosphere.

Sample phases $\delta\phi_f$ (f = 10.2 or 13.6 kHz), required for computing the frequency cross-correlation, Eq. B-1, are obtained by employing the commonly-used deterministic VLF signal propagation prediction model, known as IPP (Refs. 14 through 16). In these computations, the non-random part of the phase

TABLE B-1

STATISTICS FOR IONOSPHERIC MODEL PARAMETERS

PARAMETER / SOLAR ILLUMINATION	HEIGHT h (km)		CONDUCTIVITY GRADIENT β (km)$^{-1}$	
	MEAN $\bar{h}$	STANDARD DEVIATION σ_h	MEAN $\bar{\beta}$	STANDARD DEVIATION σ_β
Day	72	2	0.3	0.05
Night	87	2	0.5	0.1

is associated with "nominal" propagation properties of the signal path assuming a quiet ionosphere. The random part of the phase, on the other hand, is assumed to be induced by spatially uniform, random changes in the quiet ionosphere.

The linearized expression for the random phase due to an assumed random change of one standard deviation in the ionospheric parameters h and β is

$$\delta\phi_f(\sigma_h, \sigma_\beta) = \phi_f(h,\beta) - \phi_f(\bar{h},\bar{\beta}) = \frac{\partial\phi_f}{\partial\bar{h}}\ \sigma_h + \frac{\partial\phi_f}{\partial\bar{\beta}}\ \sigma_\beta \qquad \text{(B-2)}$$

where

$$h = \bar{h} + \sigma_h$$
$$\beta = \bar{\beta} + \sigma_\beta \qquad \text{(B-3)}$$

The phase of a propagating signal is approximated by

$$\phi_f(h,\beta) = \gamma_f(h,\beta)\ d + \arg\ [\Lambda_f(h,\beta)] \qquad \text{(B-4)}$$

where

$\gamma_f = \frac{2\pi f}{c}\ (1-v/c)$

f is the frequency

c is the speed of light in free space

$v_f = v_f(h,\beta)$ is the signal phase velocity

d is the signal path length

$\arg\ \Lambda_f$ is the argument (or phase) of the signal excitation factor.

Combining Eqs. B-2 and B-4 gives

$$\delta\Phi_f(\sigma_h,\sigma_\beta) = [a_f(\sigma_h,\sigma_\beta)]\, d + b_f(\sigma_h,\sigma_\beta) \qquad \text{(B-5)}$$

where

$$a_f(\sigma_h,\sigma_\beta) = \frac{\partial \gamma_f}{\partial h}\,\sigma_h + \frac{\partial \gamma_f}{\partial \beta}\,\sigma_\beta \qquad \text{(B-6)}$$

$$b_f(\sigma_h,\sigma_\beta) = \frac{\partial(\arg\Lambda_f)}{\partial h}\,\sigma_h + \frac{\partial(\arg\Lambda_f)}{\partial \beta}\,\sigma_\beta \qquad \text{(B-7)}$$

Note that Eq. B-5 is derived by assuming constant (i.e., uniform) random ionospheric parameter changes (or irregularities) along the entire signal path length d. If, however, the ionospheric irregularity does not extend over the entire signal path, d in Eq. B-4 should be replaced by the actual irregularity length. Furthermore, the excitation factor phase contribution, b_f, should be (1) multiplied by 0.5 if the irregularity covers either the transmitter or receiver alone, or (2) zero if the irregularity covers neither the transmitter nor the receiver. Assuming that the ionospheric irregularity covers the entire path, the equation for the cross-frequency correlation coefficient becomes

$$\rho_{10.2,13.6} = \frac{(a_{10.2}\, a_{13.6})\, d^2 + (b_{10.2}\, b_{13.6})}{(a_{10.2}^2\, d^2 + b_{10.2}^2)^{1/2}(a_{13.6}^2\, d^2 + b_{13.6}^2)^{1/2}} \qquad \text{(B-8)}$$

The correlation coefficient has been computed for both day and night conditions over the four different propagation paths identified in Table B-2. These paths were specifically chosen to characterize the range of propagation path properties expected along the Omega signal paths of interest in the Alaska/Yukon region.

TABLE B-2
PROPAGATION PATH PROPERTIES

PATH IDENTIFICATION \ AVERAGE PATH PROPERTIES	GROUND CONDUCTIVITY (mhos/m)	BEARING ANGLE (deg)	GEOMAGNETIC LATITUDE (deg)
I	4	0	45
II	10^{-2}	0	45
III	10^{-5}	0	45
IV	10^{-2}	-90	45

Table B-3 presents the random phase terms, a_f (Eq. B-6) and b_f (Eq. B-7) corresponding to assumed random changes (1σ) in the ionospheric parameters (given in Table B-1) for each of the four propagation paths identified in Table B-2 at 10.2 and 13.6 kHz. The results in Table B-3 indicate that the sign of either coefficient, a_f or b_f, is not altered when f changes from 10.2 to 13.6 kHz. This means that both terms in the numerator of the correlation coefficient, Eq. B-8, are positive, and the correlation coefficient is positive. Furthermore, since b_f is much less than $a_f d$ for d greater than 100 km, the results show that for signal length d greater than 100 km, the random phase can be approximated by

$$\delta\phi_{rf} \simeq a_f\, d \qquad \text{(B-9)}$$

TABLE B-3
COMPUTED VALUES OF COEFFICIENTS a_f AND b_f

T-3445

PROPAGATION PATH IDENTIFICATION	a_f (rad/km^2)				b_f (rad)			
	DAY		NIGHT		DAY		NIGHT	
	f* = 10.2	f = 13.6	f = 10.2	f = 13.6	f = 10.2	f = 13.6	f = 10.2	f = 13.6
I	-10^{-4}	-10^{-4}	-3.2×10^{-5}	-4.3×10^{-5}	-1.1×10^{-2}	-1.4×10^{-2}	-1.4×10^{-2}	-3.2×10^{-2}
II	-10^{-4}	-10^{-4}	-3.1×10^{-5}	-3.8×10^{-5}	-7.5×10^{-3}	-1.5×10^{-2}	-1.3×10^{-2}	-3×10^{-2}
III	-3.8×10^{-4}	-3.5×10^{-4}	6.6×10^{-5}	6.4×10^{-5}	1.32	3.2×10^{-1}	-3.4×10^{-2}	-3×10^{-1}
IV	-1.1×10^{-4}	-10^{-4}	8.5×10^{-6}	5.4×10^{-6}	-3.5×10^{-3}	-7.5×10^{-3}	3.5×10^{-3}	3×10^{-2}

*f is the frequency in kHz

Thus, for signal path lengths greater than 100 km, the correlation coefficient is approximately equal to

$$\rho_{10.2,13.6} \simeq \frac{a_{10.2}\, a_{13.6}\, d^2}{a_{10.3}\, a_{13.6}\, d^2} = 1 \qquad \text{(B-10)}$$

Both Eqs. B-9 and B-10 also hold even if the irregularity is smaller than the signal path length, but both the signal path and irregularity are longer than 100 km.

In conclusion, the analysis presented herein indicates that the cross-frequency correlation between 10.2 and 13.6 kHz signal random phases in Alaska is positive and approaches unity if both the signal path length and the random ionosphere irregularity length are greater than 100 km.

APPENDIX C
TRACOR 7620 NAVIGATION SET PERFORMANCE ANALYSIS

C.1 TRACOR FILTER

C.1.1 Introduction

The TRACOR Omega navigation algorithm (Ref. 17) employs a discrete-time position filter. Using a true airspeed indicator and true heading information, the algorithm propagates a dead-reckoned position on a 1.25 sec cycle. On a 10-sec cycle, Omega signals are used to provide external updates to the system. The mechanization is similar to that of a Kalman filter in that it is a recursive estimator. However, it is suboptimal, since the update gain matrix is not dependent on the computed current error covariance.

Error equations are presented for the TRACOR 7620 navigation filter. By transformation into the Z domain (Ref. 19), certain characteristics of the system may be examined analytically. Among these are system stability, damping, and state variable coupling. This transform approach also permits analysis of the statistical response of the system to Omega phase measurement errors. The power spectral density matrix, which is the transform of the error correlation matrix, is presented analytically.

C.1.2 Filter Error Equations

The filter equations may be written in 10-sec difference form as

$$\underline{\hat{x}}(kT^-) = \begin{bmatrix} 1 & 0 & 10 & 0 \\ 0 & 1 & 0 & 10 \\ 0 & 0 & 1 & 0 \\ 0 & 0 & 0 & 1 \end{bmatrix} \underline{\hat{x}}(kT-T) + \frac{10}{3600R_e} \begin{bmatrix} \cos(TH(kT-T)) \\ \frac{\sin(TH(kT-T))}{\cos(LAT(kT-T))} \\ 0 \\ 0 \end{bmatrix} TAS(kT-T) \tag{C-1}$$

and

$$\underline{\hat{x}}(kT^+) = \underline{\hat{x}}(kT^-) + K[\underline{z} - \underline{\phi}_c(\underline{\hat{x}}(kT^-))] \tag{C-2}$$

where kT^- and kT^+ are the time immediately before and after updates are incorporated.

The state estimate is

$$\underline{\hat{x}} = [\hat{LAT}, \hat{LON}, \hat{WIND}_N, \hat{WIND}_E]^T \tag{C-3}$$

in radians and radians/sec, as appropriate, and

$\underline{\phi}_c(\underline{\hat{x}})$ is the vector of nominal Omega composite predictions in cycles

$\underline{z}$ is the vector of Omega composite measurements

$\underline{v}$ is the vector of Omega phase measurement errors

TH is true heading

TAS is true airspeed in knots

R_e is the radius of the earth in nautical miles

T is the time interval, 10 sec.

The form of the gain matrix K is

$$K = P_f \, H(\underline{\hat{x}}) R_f^{-1} \tag{C-4}$$

where P_f and R_f^{-1} are fixed matrices. The measurement matrix H can be used to approximate the difference between Omega predictions and measurements:

$$\underline{z} - \underline{\phi}_c(\underline{\hat{x}}) = H(\underline{\hat{x}}) \, [\underline{\hat{x}} - \underline{x}] \tag{C-5}$$

including Andoyer-Lambert ellipticity corrections. (For simplicity, the functional notation $H(\underline{\hat{x}})$ is dropped hereafter and only H is used.)

By employing direct perturbation and combining the above equations, it can be shown that the error equations are

$$\underline{\Delta x}(kT) = [I - KH] \{\Phi \underline{\Delta x}(kT-T) + L[\underline{w}(kT-T) - \underline{w}(kT)] + G \, \underline{v}_m(kT)\} + K \, \underline{v}(kT) \tag{C-6}$$

where the true wind vector is

$$\underline{w} = [WIND_N, \, WIND_E]^T \tag{C-7}$$

the instrument error vector is

$$\underline{v}_m = [\Delta TAS, \, \Delta TH]^T \tag{C-8}$$

Omega measurement error is described by $\underline{v}$ and the transition matrix is

$$\Phi = \begin{bmatrix} 1 & 0 & 10 & 0 \\ f & 1 & 0 & 10 \\ 0 & 0 & 1 & 0 \\ 0 & 0 & 0 & 1 \end{bmatrix} \qquad \text{(C-9)}$$

where

$$f = -10\ TAS\ \sin(TH)\ \sec(LAT)\ \tan(LAT)/3600R_e \qquad \text{(C-10)}$$

$$L = \begin{bmatrix} 10 & 0 & 1 & 0 \\ 0 & 10 & 0 & 1 \end{bmatrix}^T \qquad \text{(C-11)}$$

and

$$G = \frac{10}{3600R_e} \begin{bmatrix} \cos(TH) & -TAS\ \sin(TH) \\ \sin(TH)\ \sec(LAT) & TAS\ \cos(TH)\ \sec(LAT) \\ 0 & 0 \\ 0 & 0 \end{bmatrix} \qquad \text{(C-12)}$$

Equations C-1 through C-5 are used in a direct simulation of the TRACOR 7620 navigation algorithm. Equation C-6 provides the error formulation required to perform statistical analysis of the filter.

C.1.3 Transform Analysis

If the measurement matrix H is held constant, Eq. C-6 can be Z-transformed (Ref. 19) and manipulated to yield

$$\underline{\Delta X}(z) = [zI - (I - KH)\Phi]^{-1} [(1 - z)(I - KH)\ L\ \underline{W}(z) + z(I - KH)\ G\ \underline{V}_m(z) + z\ K\underline{V}(z)] \qquad \text{(C-13)}$$

Although H is geometry-dependent, it tends to change slowly at moderate aircraft speeds. Consequently, this transform of the "snapshot" gives a good representation of error behavior, and should yield considerable insight into system behavior for other flight profiles.

The system characteristic function was calculated for Inuvik, assuming availability of signals from stations A, C, D and H; the result is

$$c(z) = z^4 - 3.17z^3 + (3.64 + 0.04f)z^2 - (1.76 + 0.04f)z + (0.29 + 0.04f) \qquad \text{(C-14)}$$

At these latitudes

$$|f| \leq 0.001$$

For f = 0, system poles are found at

$$z_1 \approx 0.35$$

$$z_2 \approx 0.96$$

$$z_{3,4} \approx 0.93 \pm j\ 0.027$$

From this analysis it is possible to conclude that

- The system is stable
- The $z_{3,4}$ pole-pair gives rise to a lightly damped oscillation
- Maneuvers, which change the value of f, will not affect system stability
- Manuevers will move the poles, creating transient errors.

C.1.4 Power Spectral Density Analysis

Given a transfer function and power spectral densities of input disturbances, it is possible to calculate the power spectral density (PSD) matrix of the error vector if the processes are stationary (Ref. 20).

Under this assumption, the PSD matrix of state error is

$$P_{xx}(s) = [zI - (I-KH)\Phi]^{-1} [|z-1|^2 (I-KH) LP_w(s) \bar{L} \overline{(I-KH)}$$

$$+ |z|^2 (I-KH) GP_m(s)\bar{G}\overline{(I-KH)} + |z|^2 KR(s)\bar{K}] \times$$

$$\overline{[z\ I - (I - KH)\Phi]^{-1}} \qquad \text{(C-15)}$$

where

$z = e^{sT}$

s is the Laplace transform variable

$P_w(s)$ is the wind PSD matrix

$P_m(s)$ is the instrument error PSD matrix

$R(s)$ is the Omega measurement error PSD matrix

$(\bar{\ })$ indicates the complex conjugate of a transposed matrix

P_{xx} is a steady-state power spectral density and does not reflect the time-varying error covariance propagation characteristics.

C.2 TRACOR FILTER WIND RESPONSE

C.2.1 Introduction

One factor contributing to position error is wind. The impact of wind on position error covariance is difficult

to determine, since relatively little is known about wind correlations in the Alaska/Yukon region.

Since the TRACOR filter carries state variables for north and east wind, a constant wind would be accurately estimated, but changing winds will induce transient errors. Since the only observations of wind are from induced Omega position error, these transients may decay slowly.

C.2.2 Winds in Alaska

Data were analyzed for surface winds at Eielson AFB, near Fairbanks, Alaska (Ref. 18); the following were noted:

- The air was calm for 50% of the observations on a year-round basis
- Wind speed was less than 10 kt for 97% of observations
- No observation was made of windspeed greater than 34 kt
- Mean scalar wind speed was 2.4 kt.

However, the relation of surface winds to wind in the upper air is not available, and the time correlation of wind speeds in different directions is unknown. As a result, the contribution of wind to position error covariance is difficult to determine.

C.2.3 Simulation of Wind Effects

In order to assess the impact of wind on position error, a number of simulations were run. The simulations whose results results are depicted in Figs. C-1 and C-2 used wind speeds of 10 kt and 50 kt, respectively. Other simulation conditions were:

- Initial position: 68°N, 134°W
- Zero initial wind
- True airspeed: 250 kt
- Signals from transmitting stations A, C, D, and H assumed to be available
- Perfect reception and monitor corrections assumed
- Initial track: 180°
- At 2 min, north wind undergoes a step change from zero to the appropriate magnitude
- At 20 min, wind direction shifts to east
- Also at 20 min, the aircraft starts to turn clockwise through 270° at 3°/sec

Figure C-1 and C-2 show the same features predicted by the transform analysis. The lightly damped oscillation is not a dominant feature of the system response. Some coupling exists between north and east position errors. Also, note that maximum radial position errors occur at 4:50* and 22:40 flight time in both simulations - 2:50 and 2:40 after wind shifts.

The difference between the results of the two simulations is in error magnitude. The maximum position errors induced by the wind errors are provided in Table C-1. Note that for this range of wind magnitudes, the TRACOR 7620 response to wind shifts is nearly linear.

Position errors induced by wind shift are important but not critical. Maximum position errors of approximately 0.23 nm per 10 kt of wind step may be expected. Should wind change more gradually, smaller maximum errors would be expec-

*(min:sec) of simulation time.

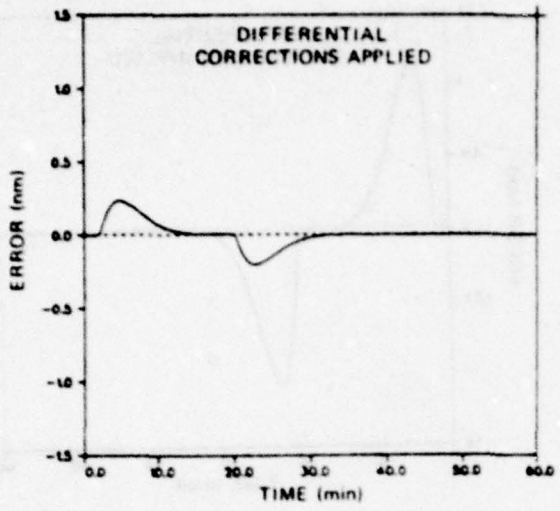

a) North Position Error

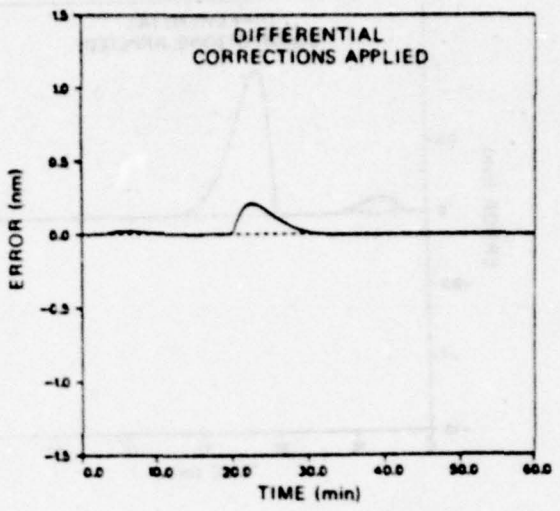

b) East Position Error

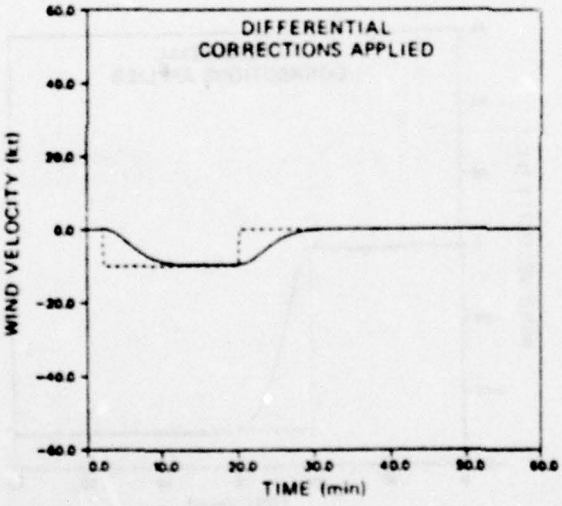

c) North Wind

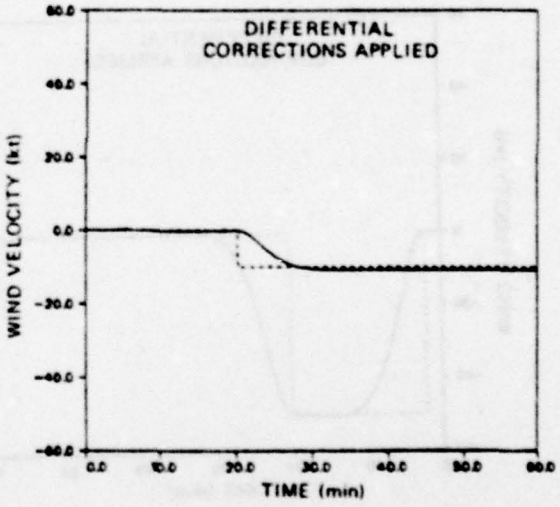

d) East Wind

Figure C-1 TRACOR 7620 Response to 10 kt Wind Shift

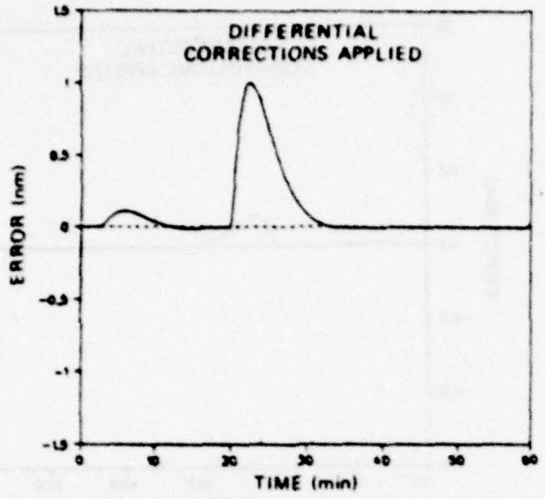

a) North Position Error

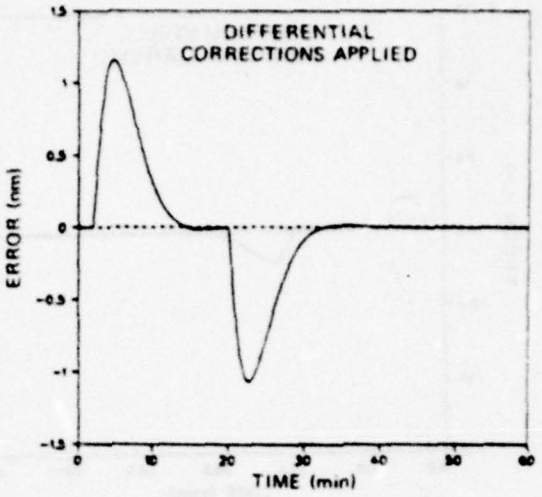

b) East Position Error

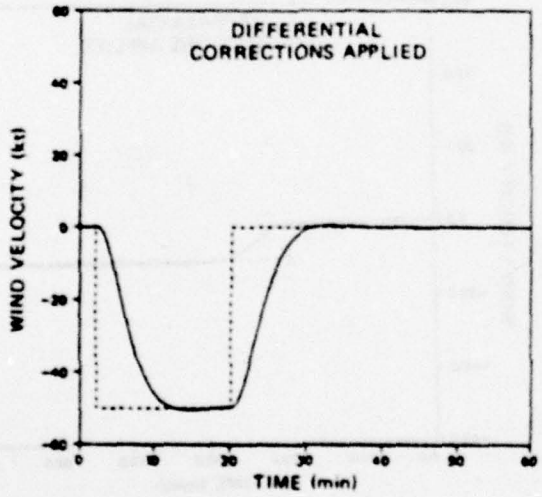

c) North Wind

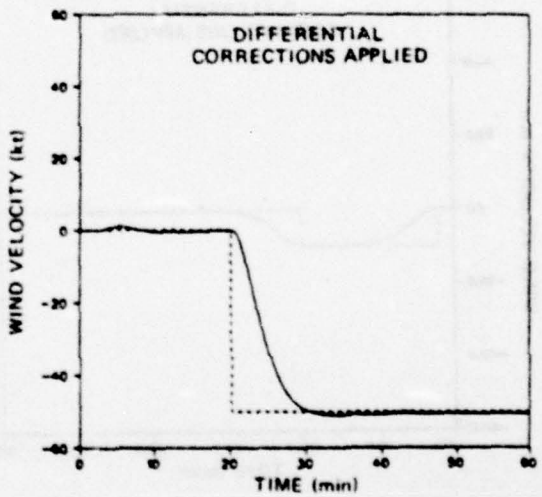

d) East Wind

Figure C-2 TRACOR 7620 Response to 50 kt Wind Shift

ted. While slower than for maneuver-induced error, transient decay still reduces position error to 10% of maximum within 10 min of the wind shift.

TABLE C-1
POSITION ERRORS DUE TO 10 kt AND 50 kt WINDS

T-3446

	10 kt WIND		50 kt WIND	
TIME (min:sec)	NORTH POSITION ERROR (nm)	EAST POSITION ERROR (nm)	NORTH POSITION ERROR (nm)	EAST POSITION ERROR (nm)
2:00	0	0	0	0
4:50	0.24	0.021	1.2	0.098
20:00	0.0080	0.0010	-0.0010	-0.0020
22:40	-0.20	0.21	-1.6	1.0

REFERENCES

1. Kasper, J.F., Jr., and Hutchinson, C.E., "Omega: Global Navigating by VLF Fix," IEEE Spectrum, Vol. 16, No. 5, May 1979, pp. 59-63.

2. Kasper, J.F, Jr., "Omega Propagation Prediction Algorithm," The Analytic Sciences Corporation, Technical Information Memorandum TIM-487-2, January 1974.

3. Simolunas, A.A., and Quinn, G.H., Alaskan Air Navigation Requirements: Volume I -- An Overview, Federal Aviation Administration, Report No. FAA-RD-76-27, I, January 1977.

4. Quinn, G.H., "LORAN-C and OMEGA in Aviation," Proceedings of the Conference on Navigation in Transportation (Cambridge), November 1978, pp. 101-109.

5. Schweppe, F.C., Uncertain Dynamic Systems, Prentice-Hall, Inc., Englewood Cliffs, N.J., 1973.

6. Federal Aviation Administration, "United States Standard for Terminal Instrument Procedures (TERPS)," FAA Handbook 8260.3B, 3rd ed., July 1976.

7. Bell, A.R., "Omega Software Evaluation," The Analytic Sciences Corporation, Technical Report TR-747-5, June 1976.

8. Federal Aviation Administration, "Approval of Area Navigation Systems for Use in the U.S. National Airspace System," Advisory Circular AC-90-45A, February 1975.

9. Beukers, J.M., "Accuracy Limitations of the Omega Navigation System Employed in the Differential Mode," Proceedings of the ION National Marine Meeting, October 1972.

10. Gelb, A. (Editor), Applied Optimal Estimation, MIT Press, Cambridge, 1974.

11. Wait, J.R., and Spies, K.P., "Characteristics of the Earth-Ionosphere Waveguide for VLF Radio Waves," NBS Technical Note No. 300, December 1964.

12. Kelly, F.J., Rhoads, F.J., and Hansen, I.P., "On Statistical Multimode VLF Field Strength Predictions," Naval Research Laboratory, NRL Report 7239, February 1971.

13. Defense Communications Agency, "Comparison of Predicted VLF/LF Signal Levels with Propagation Data," Report No. 960-TP-74-5, January 1974.

14. Ferguson, J.A., "A Report on the Integrated Prediction Program with Nuclear Environment (IPP-2)," Naval Electronics Laboratory Center, Technical Note TN1890, July 1971.

15. Donnelly, S.F., "Integrated Propagation Prediction Program Documentation," The Analytic Sciences Corporation, Technical Report TR-343-4, November 1973.

16. Gupta, R.R., "Theoretical Background of IPP-2," The Analytic Sciences Corporation, Technical Report TR-343-2, February 1973.

17. TRACOR, Inc., "Prime Item Development Specification and Computer Program Development Specification, Omega Navigation Equipment (ONE)," Vol. V, Report No. RFP-F33657-75-R-0417, April 1975.

18. "Revised Uniform Summary of Surface Weather Observations, Part C, Eielson AFB," Data Processing Branch, USAF Environmental Technical Applications Center, June 1978.

19. Cadzow, J.A., Discrete-Time Systems, Prentice-Hall, Inc., Englewood Cliffs, N.J., 1973.

20. Wozencraft, J.M., and Jacobs, I.M., Principles of Communication Engineering, John Wiley and Sons, New York, 1965.